

Additive quantile regression for clustered data with an application to children's physical activity

Marco Geraci*

Abstract: Additive models are flexible regression tools that handle linear as well as nonlinear terms. The latter are typically modelled via smoothing splines. Additive mixed models extend additive models to include random terms when the data are sampled according to cluster designs (e.g., longitudinal). These models find applications in the study of phenomena like growth, certain disease mechanisms and energy consumption in humans, when repeated measurements are available. In this paper, we propose a novel additive mixed model for quantile regression. Our methods are motivated by an application to physical activity based on a dataset with more than half million accelerometer measurements in children of the UK Millennium Cohort Study. In a simulation study, we assess the proposed methods against existing alternatives.

MSC 2010 subject classifications: Primary 62J99; secondary 62G08.

Keywords and phrases: bag of little bootstraps, linear quantile mixed models, low rank splines, random effects, shrinkage, smoothing.

1. Introduction

The goal of regression analysis is to model the distribution of an outcome as a function of one or more covariates. Mean regression is used to assess how the outcome changes on average when the covariates change, and often implies that the direction and strength of the statistical associations are the same for all individuals in a population. However, conditionally on their observed characteristics, subjects who rank below or above the average of the outcome distribution may respond differently to the same treatment or exposure. Evidence of heterogeneous effects across the outcome distribution have been found in countless research including the effect of smoking on weight in lighter or heavier infants (Abrevaya, 2001; Koenker and Hallock, 2001; Geraci, 2016a); the effect of succimer chelation on different levels of cadmium concentrations in children's blood (Cao et al., 2013); or the effect of sedentary behavior and food prices on different centiles of children's anthropometric variables (España Romero et al., 2013; Sturm and Datar, 2005). These children may be at higher risks of morbidity and mortality than those who are at the center of the distribution.

By definition, mean effects average out stronger and weaker effects. The averaging may even cancel out symmetric effects of same magnitudes but opposite

*Department of Epidemiology and Biostatistics, Arnold School of Public Health, University of South Carolina, 915 Greene Street, Columbia SC 29209, USA. e-mail: geraci@mailbox.sc.edu

signs on the tails of the distribution. Quantile regression (QR) (Koenker and Bassett, 1978) is a flexible statistical tool with a vast number of applications that complements mean regression. QR has become a successful analytic method in many fields of science because of its ability to draw inferences about individuals that rank below or above the population conditional mean. The ranking within the conditional distribution of the outcome can be considered as a natural index of individual latent characteristics which cause heterogeneity at the population level (Koenker and Geling, 2001). There is an increasingly wider acknowledgement of the importance of investigating sources of heterogeneity to quantify more accurately costs, benefits, and effectiveness of interventions or medical treatments, whether it be an after-school physical activity program, a health care reform, or a thrombolytic therapy (see, for example, Austin et al., 2005; Beets et al., 2016; Beyerlein, 2014; Ding et al., 2010; Rehkopf, 2012; Wei and Terry, 2015; Winkelmann, 2006). QR is particularly suitable for this purpose as it yields inferences that are valid regardless of the true underlying distribution. Also, quantiles enjoy a number of properties (Gilchrist, 2000), including equivariance to monotone transformations and robustness to outliers.

In this paper we are concerned specifically with nonparametric quantile regression functions of continuous response variables when data arise from cluster designs. Our research is motivated by a study on daily and weekly physical activity patterns in school-aged children using high-frequency accelerometer data. In general, temporal (diurnal) trajectories of physical activity are characterized by strongly nonlinear patterns that require some degree of smoothing (Butte, Ekelund and Westerterp, 2012; Fan et al., 2015; Morris et al., 2006; Sera et al., 2011, 2017). On the other hand, some predictors of interest may simply have linear effects. If, in addition, data are collected longitudinally to examine weekly patterns, then the correlation at the individual level must be taken into account.

We propose novel additive quantile models that include linear terms, nonlinear terms, as well as random-effects terms which account for the clustering. Further, nonlinear terms are modelled nonparametrically using penalized splines and fitted via automatic scatterplot smoothing within a mixed model framework (Ruppert, Wand and Carroll, 2003). In the next section, we briefly describe the data. In Section 3, we describe the state of the art in nonlinear quantile regression and highlight the differences between our proposal and existing, potentially competing approaches. In Section 4, we describe the methods and, briefly, their implementation in the R language (R Core Team, 2014), with further technical details provided in Appendix A. In Section 5, we carry out a simulation study to assess the performance of the proposed methods (with tables reported in Appendix B). The real data analysis is presented in Section 6 while concluding remarks are given in Section 7.

2. Sedentariness and physical activity in UK children

The benefits of regular physical activity on well-being and life expectancy as well as the detrimental health effects of sedentary behavior have been amply

documented (e.g., see [Ekelund et al., 2016](#); [Katzmarzyk and Pate, 2017](#); [Warburton, Nicol and Bredin, 2006](#)). Physical inactivity in England is estimated to cost more than eight billion pounds a year. This includes both the direct costs of treating major, lifestyle-related diseases and the indirect costs of sickness absence ([National Institute for Health and Clinical Excellence, 2008](#)). It is also estimated that 54,000 premature deaths a year are linked to a sedentary lifestyle ([Department for Culture, Media and Sport, 2002](#)).

Since establishing an active lifestyle at an early age is an important form of prevention against morbidity and premature mortality, promotion of physical activity in children and young people has gained a strategically central place in the public health agenda ([National Institute for Health and Clinical Excellence, 2009](#)). A nationally representative study ([Griffiths et al., 2013a](#)) showed that only half of UK seven-year-olds achieve recommended levels of physical activity, with girls far less active than boys. It is therefore important to identify the predictors of physical activity, not only at the average intensity of activity but also (and perhaps especially) at lower and upper intensities.

Accelerometer data collected in seven-year-old children of the Millennium Cohort Study (MCS), a UK-wide longitudinal multi-purpose survey, represent a major, large-scale epidemiological resource to study physical activity determinants ([Griffiths et al., 2013b](#)). Accelerometers are devices capable of providing an objective measure of the intensity and duration of movement. They produce an output known as ‘acceleration counts’ which is dimensionless and thus requires calibration in order to be converted into physiologically more relevant units, usually based on energy expended per unit of time (e.g., metabolic equivalent of task). The plot in Figure 1 shows accelerometer counts by time of the day for a subset of MCS children who provided reliable data for 7 days of the week. Since temporal trajectories of activity were similar between Monday and Friday, and during Saturday and Sunday, data in the plot are shown for weekdays (or workdays) and weekend days, respectively. Each dot represents the accelerometer counts measured on any of the weekdays or weekend days for a child at a given time of the day, while the solid lines are piecewise linear curves connecting sample quantiles estimated cross-sectionally (conditional on time). During weekdays there are periods of higher activity levels that mirror traveling times to and from school, and lunch and break times ([Sera et al., 2017](#)). However, temporal trajectories at different quantile levels of the conditional distribution are not simply vertical shifts of one another. This suggests that the scale and possibly the shape of the counts distribution change with time of the day. For example, the skewness of the distribution in the weekend is small early in the morning, and steadily increases during the day.

3. Approaches to nonlinear quantile regression

Nonlinear associations occur in many research studies, including bioassays and pharmacokinetic experiments ([Lindsey, 2001](#)), as well studies related to growth processes in biology and agriculture ([Davidian and Giltinan, 2003](#)). In the presence of nonlinearity, there are different modelling strategies one may consider.

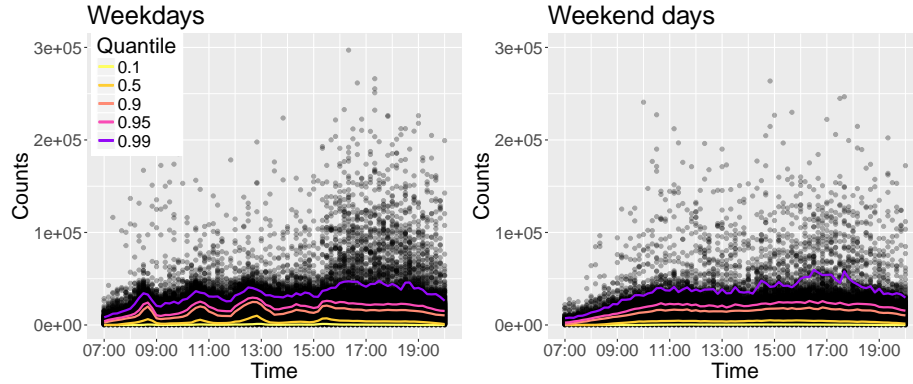


FIGURE 1. Accelerometer counts (rounded to the nearest 100) observed between 7:00 and 20:00 and aggregated over 10-minute intervals in 1154 English children of the UK Millennium Cohort Study, by days of the week (Monday through Friday, weekdays; Saturday and Sunday, weekend). Solid lines connect sample quantiles that are estimated conditionally on time for 5 quantile levels (0.1, 0.5, 0.9, 0.95, 0.99).

Nonparametric models, smoothing splines (including polynomial models), and transformation models are the most commonly adopted. In addition to the specific strategy, one must also take into account the particular analytical framework: for example, is the sampling design cross-sectional or longitudinal? Is the outcome discrete or continuous? Should distributional assumptions be parametric or nonparametric? And so on. The effort needed for the analysis may have, at times, considerable weight on the final decision regarding which approach to follow. Lack of theory or even computer software can move the needle towards one choice over another.

The literature on parametric and nonparametric nonlinear regression models is vast. However, most of the work has been done in relation to nonlinear mean regression. In comparison, substantially less methods have been developed for nonlinear quantile regression and even less for nonlinear quantile regression with clustered data. A brief account of strategies to nonlinear quantile regression modelling is given by Geraci (2016b) and these consist in: (i) smoothing (nonparametric regression); (ii) nonlinear parametric models; and (iii) transformation models. In the next sections, we discuss methods that fall in the first group and that are of direct relevance to the present study, and briefly survey those in the other two groups for completeness.

3.1. Nonparametric models

Nonparametric regression and, more in general, additive models occupy an important place in statistical modelling. Popular approaches include locally weighted scatterplot smoothing (Cleveland, 1979; Cleveland and Devlin, 1988) and smoothing splines (Wahba, 1990; de Boor, 2001; Hastie and Tibshirani,

1990; Ruppert, Wand and Carroll, 2003). If we consider the literature on nonparametric quantile functions for data with no clustering, there is a considerable variety of proposals. For example, Koenker, Ng and Portnoy (1994), He, Ng and Portnoy (1998), Koenker and Mizera (2004), and Koenker (2011) considered total variation roughness penalties for univariate, bivariate, and additive quantile smoothing splines. For smooth functions, the total variation penalty corresponds to the L_1 counterpart of the L_2 smoothing spline penalty and leads to an elegant, computationally convenient optimization problem which can be solved via linear programming (Koenker and Mizera, 2004). Yu and Jones (1998), Horowitz and Lee (2005), and Spokoiny, Wang and Härdle (2013) proposed estimation methods based on kernel weighted and polynomial local linear fitting. Other, similar local fitting methods are given in Wu, Yu and Yu (2010) and Cai and Xu (2008). In the Bayesian framework for independent data, Thompson et al. (2010) proposed an approach based on natural cubic splines (Green and Silverman, 1994) with a Gaussian smoothness prior.

A few approaches have been proposed also for the estimation of nonparametric quantile functions with repeated measurements or when the data are subject to other forms of dependence. Wei et al. (2006) considered modelling and estimation of longitudinal growth curves. They discussed an additive quantile regression model decomposed into a nonparametric temporal trend, a first-order autoregressive component, and a partially linear component to adjust for other covariates. Fenske et al. (2013) extended Fenske, Kneib and Hothorn's (2011) method to additive quantile regression based on longitudinal data. In their model, fitted via boosting, they included L_2 -penalized fixed cluster-specific intercepts and slopes (thus, no covariance structure) with pre-specified shrinkage parameters, to account for individual deviations from a 'population' trend. Additive nonlinear effects were modelled via penalized splines, again, with pre-specified amount of smoothing as controlled by the number of boosting iterations. An additive model is also considered by Yue and Rue (2011) who proposed normally distributed random intercepts and nonlinear terms with Bayesian P-splines and Gaussian Markov random fields as smoothness priors. Finally, it is worth mentioning that a related, although different, approach involves modelling the quantile regression coefficients in varying coefficient models, such as those by Andriyana, Gijbels and Verhasselt (2014) and Reich, Fuentes and Dunson for, respectively, longitudinally and spatially correlated data.

The modelling approach we develop in this study differs on several accounts from existing proposals. First of all, we model the intra-cluster correlation by means of random effects instead of autoregressive errors (Wei et al., 2006). Secondarily, in contrast to Yue and Rue (2011), we include cluster-specific random slopes in addition to random intercepts, and, in contrast to Fenske et al. (2013), we allow cluster-specific effects to have a general covariance matrix. In addition, our estimation approach radically differs from that of Fenske et al. (2013) since, as described in Section 4, the optimal degree of shrinkage of the cluster-specific effects and the optimal level of smoothing for the nonlinear terms are automatically estimated from the data.

3.2. Nonlinear parametric models

Contributions to statistical methods for nonlinear mean regression when data are clustered can be found in the literature of mixed-effects modelling (Lindstrom and Bates, 1990; Pinheiro and Bates, 1995, 2000) as well as generalized estimating equations (Davidaian and Giltinan, 1995, 2003; Contreras and Ryan, 2000; Vonesh et al., 2002). In contrast, there seem to be only a handful of published articles in the statistical literature on *parametric* nonlinear quantile regression functions with clustered data. Karlsson (2008) considered nonlinear longitudinal data and proposed weighting the standard quantile regression estimator (Koenker and Bassett, 1978) with pre-specified weights. Wang (2012), taking her cue from Geraci and Bottai (2007), used the AL distribution to define the likelihood of a Bayesian nonlinear quantile regression model. Huang and Chen (2016) proposed a Bayesian joint model for time-to-event and longitudinal data. An approach based on copulas is developed by Chen, Koenker and Xiao (2009). Oberhofer and Haupt (2016) established the consistency of the L_1 -norm nonlinear quantile estimator under weak dependency. Finally, Geraci (2017a) extended Geraci and Bottai's (2014) quantile mixed models to the nonlinear case.

3.3. Transformation models

Traditionally, transformations toward linearity have been developed for conditional mean function estimation (e.g. Aranda-Ordaz, 1981; Box and Cox, 1964), with some proposals to deal with clustered data (see, for example, Gurka et al., 2006; Hutmacher et al., 2011; Maruo et al., 2017). This general approach has been taken by others in quantile function estimation when data are independent using the Box-Cox transformation (Buchinsky, 1995; Chamberlain, 1994; Mu and He, 2007), the Aranda-Ordaz transformation (Dehbi, Cortina-Borja and Geraci, 2016), as well as other new flexible transformations (Geraci and Jones, 2015). In particular, Mu and Wei (2009) developed a Box-Cox quantile regression model with varying coefficients for longitudinal data.

4. Methods

4.1. Notation

We consider data from two-level nested designs in the form $(\mathbf{x}_{ij}^\top, \mathbf{z}_{ij}^\top, y_{ij})$, for $j = 1, \dots, n_i$ and $i = 1, \dots, M$, $N = \sum_i n_i$, where \mathbf{x}_{ij}^\top is the j th row of a known $n_i \times p$ matrix \mathbf{X}_i , \mathbf{z}_{ij}^\top is the j th row of a known $n_i \times q$ matrix \mathbf{Z}_i and y_{ij} is the j th observation of the response vector $\mathbf{y}_i = (y_{i1}, \dots, y_{i n_i})^\top$ for the i th unit or cluster. This kind of data arise from longitudinal studies and other cluster sampling designs (e.g., spatial cluster designs). Throughout the paper, the covariates x and z are assumed to be given and measured without error. The $n \times 1$ vector of zeros and ones will be denoted by, respectively, $\mathbf{0}_n$ and

$\mathbf{1}_n$, the $n \times n$ identity matrix by \mathbf{I}_n , and the $m \times n$ matrix of zeros by $\mathbf{O}_{m \times n}$. Finally, the Kronecker product and the direct sum will be denoted by \otimes and \oplus , respectively.

4.2. The model

We define the following τ th additive quantile regression model

$$Q_{y_{ij}|\mathbf{u}_i, \mathbf{x}_i, \mathbf{z}_i}(\tau) = \beta_{\tau,0} + \sum_{k=1}^p g_{\tau}^{(k)}(x_{ijk}) + \mathbf{z}_{ij}^{\top} \mathbf{u}_{\tau,i}, \quad j = 1, \dots, n_i, \quad i = 1, \dots, M, \quad (1)$$

for $\tau \in (0, 1)$, where $g_{\tau}^{(k)}$ is a τ -specific, centered, twice-differentiable, smooth function of the k th component of \mathbf{x} . The $q \times 1$ vector $\mathbf{u}_{\tau,i}$ collects cluster-specific random effects associated with \mathbf{z}_{ij} and its distribution is assumed to depend on a τ -specific parameter (further details are provided in the next section).

Without loss of generality, let the components of $\mathbf{x} = (x_1, \dots, x_s, x_{s+1}, \dots, x_p)^{\top}$ be ordered in such a way that the first s terms of the summation in (1) are nonlinear functions and the remaining $p-s$ are linear. To model nonlinear functions, we consider a spline model of the type

$$g_{\tau}(x) \approx \sum_{h=1}^H v_{\tau,h} B_h(x),$$

(e.g., cubic or B-Spline), where the B_h 's and $v_{\tau,h}$'s, $h = 1, \dots, H$, denote, respectively, the basis functions and the corresponding coefficients, and H depends on the degrees of freedom or the number of knots. Note that the coefficients are τ -specific. The quantile function in (1) is then approximated by

$$Q_{y_{ij}|\mathbf{u}_i, \mathbf{x}_i, \mathbf{z}_i}^*(\tau) = \beta_{\tau,0} + \sum_{k=1}^s \sum_{h=1}^{H_k} v_{\tau,hk} B_h^{(k)}(x_{ijk}) + \sum_{k=s+1}^p \beta_{\tau,k} x_{ijk} + \mathbf{z}_{ij}^{\top} \mathbf{u}_{\tau,i}. \quad (2)$$

Let $\mathbf{B}^{(k)}(x_{ijk})$ be the $H_k \times 1$ vector of values taken by the k th spline evaluated at x_{ijk} , $\mathbf{v}_{\tau,k} = (v_{\tau,1}, \dots, v_{\tau,H_k})^{\top}$ be the $H_k \times 1$ vector of spline coefficients for the k th covariate, and $H = \sum_k H_k$. Further, define \mathbf{B}_i as the $n_i \times H$ matrix with rows $(\mathbf{B}^{(1)}(x_{ij1})^{\top}, \dots, \mathbf{B}^{(s)}(x_{ijs})^{\top})^{\top}$, $j = 1, \dots, n_i$, and let $\mathbf{v}_{\tau} = (\mathbf{v}_{\tau,1}^{\top}, \dots, \mathbf{v}_{\tau,s}^{\top})^{\top}$. With a slight abuse of notation, we write (2) for the i th cluster in matrix form as

$$Q_{\mathbf{y}_i|\mathbf{u}_i, \mathbf{x}_i, \mathbf{z}_i}^*(\tau) = \mathbf{F}_i \boldsymbol{\beta}_{\tau} + \mathbf{Z}_i \mathbf{u}_{\tau,i} + \mathbf{B}_i \mathbf{v}_{\tau}, \quad i = 1, \dots, M, \quad (3)$$

where \mathbf{F}_i is the $n_i \times (p-s+1)$ matrix with rows $(1, x_{ij(s+1)}, \dots, x_{ijp})^{\top}$, $j = 1, \dots, n_i$, and $\boldsymbol{\beta}_{\tau} = (\beta_{\tau,0}, \beta_{\tau,s+1}, \dots, \beta_{\tau,p})^{\top}$. We call (3) an additive linear quantile mixed model, or AQMM for short.

The additive model introduced above opens up the question on how to control the trade-off between bias and efficiency, and, thus, the degree of smoothness of the estimate. At this juncture of our paper, we take a detour to briefly introduce the well-known link existing between penalized splines and mixed-effect models (see, e.g., [Ruppert, Wand and Carroll, 2003](#), for an excellent review of this topic). Consider the following regression spline model

$$\mathbf{y} = \mathbf{X}\boldsymbol{\beta} + \mathbf{B}\mathbf{v} + \boldsymbol{\epsilon}$$

for some $n \times p$ design matrix \mathbf{X} and $n \times H$ basis matrix \mathbf{B} , where \mathbf{y} is a vector of observations and $\boldsymbol{\epsilon}$ is a vector of independent and identically distributed (IID) normal errors $\mathcal{N}(0, \sigma^2)$ of dimension n . Penalized estimation of \mathbf{v} can be carried out by minimizing the objective function

$$\|\mathbf{y} - \mathbf{X}\boldsymbol{\beta} - \mathbf{B}\mathbf{v}\|^2 + \lambda \|\mathbf{v}\|_{\mathbf{D}}^2$$

where $\lambda \geq 0$ is the *smoothing parameter* and $\mathbf{D} = \mathbf{I}_H$. The above objective function, rescaled by σ^2 , is equivalent to the best linear unbiased prediction criterion of the linear mixed-effects model $\mathbf{y} = \mathbf{X}\boldsymbol{\beta} + \mathbf{B}\mathbf{v} + \boldsymbol{\epsilon}$ with $\mathbf{v} \sim \mathcal{N}(\mathbf{0}, \sigma_v^2 \mathbf{I})$, $\sigma_v^2 = \sigma^2/\lambda$, and $\boldsymbol{\epsilon} \sim \mathcal{N}(\mathbf{0}, \sigma^2 \mathbf{I})$. Since the variance σ_v^2 is estimated from the data, it follows that the degree of smoothing is *automatically* chosen by the estimation algorithm.

Automatic smoothing selection does not necessarily lead to optimal smoothing ([Ruppert, Wand and Carroll, 2003](#)). However, one of the advantages of working with random spline coefficients when modelling cluster data is that \mathbf{v} can be subsumed in the random part of the model containing the cluster-specific effects. Choice of the ‘prior’ distribution for \mathbf{v} effectively corresponds to choosing the form of the penalty. One approach is to use the same metric for the penalty term as that for the fidelity term. The L_1 -penalty, which is linked to the double exponential distribution ([Geraci and Bottai, 2007, 2014](#)), is sometimes used in quantile regression models due to its computational convenience ([Koenker, Ng and Portnoy, 1994](#); [Koenker and Mizera, 2004](#)). The resulting smoothed curves are piecewise linear and are most useful in the presence of breakpoints, sharp bends, and spikes ([Koenker and Mizera, 2004](#)).

In contrast, the L_2 -penalty represents a more suitable choice for modelling smooth changes as in, for example, variations of energy expenditure over time. This is, for example, the approach considered by Cox and Jones in the discussion of [Cole \(1988\)](#) who suggested the spline smoothing quantile regression model

$$\rho_\tau(y - f(x)) + \lambda \int \{f''(x)\}^2 dx,$$

where $\rho_\tau(r) = r \{ \tau - I(r < 0) \}$ is the quantile regression check function ([Koenker and Bassett, 1978](#)) and I denotes the indicator function. As compared to other roughness functionals, this kind of penalty yields a more visually appealing form of smoothness.

A natural link between L_2 -penalized splines and random effects is provided by the normal distribution. Hence, in our random-effects specification of (3), we

assume that the vectors $\mathbf{u}_{\tau,i}$ and \mathbf{v}_{τ} follow zero-centered multivariate Gaussians with variance-covariance matrices $\boldsymbol{\Sigma}_{\tau}$ and $\boldsymbol{\Phi}_{\tau} = \bigoplus_{k=1}^s \phi_{\tau,k} \mathbf{I}_{H_k}$, respectively. Further, we assume that the $\mathbf{u}_{\tau,i}$'s are independent for different i (but may have a general covariance structure) and are independent from \mathbf{v}_{τ} . Our objective function is then given by

$$\sum_{i=1}^M \rho_{\tau} (\mathbf{y}_i - \mathbf{F}_i \boldsymbol{\beta}_{\tau} - \mathbf{Z}_i \mathbf{u}_{\tau,i} - \mathbf{B}_i \mathbf{v}_{\tau}) + \sum_{i=1}^M \|\mathbf{u}_{\tau,i}\|_{\boldsymbol{\Sigma}_{\tau}^{-1}}^2 + \sum_{k=1}^s \phi_{\tau,k}^{-1} \|\mathbf{v}_{\tau,k}\|^2, \quad (4)$$

with the convention that $\rho_{\tau}(\mathbf{r}) = \sum_{j=1}^n r_j \{\tau - I(r_j < 0)\}$ for a vector $\mathbf{r} = (r_1, \dots, r_n)^{\top}$. Note that the $\phi_{\tau,k}$'s determine the amount of smoothing for the nonparametric terms.

4.3. Inference

The minimization of (4) is equivalent to fitting a linear quantile mixed model (LQMM) (Geraci and Bottai, 2007, 2014) where the asymmetric Laplace density

$$p(y) = \frac{\tau(1-\tau)}{\sigma_{\tau}} \exp \left\{ -\frac{1}{\sigma_{\tau}} \rho_{\tau}(y - \mu_{\tau}) \right\},$$

with location $\mu_{\tau} \in \mathbb{R}$ and scale $\sigma_{\tau} > 0$, is employed as quasi-likelihood for the fidelity term.

Define $\mathbf{y} = (\mathbf{y}_1^{\top}, \dots, \mathbf{y}_M^{\top})^{\top}$ and $\mathbf{u}_{\tau} = (\mathbf{u}_{\tau,1}^{\top}, \dots, \mathbf{u}_{\tau,M}^{\top})^{\top}$. Let $\boldsymbol{\theta}_{\tau} \equiv (\boldsymbol{\beta}_{\tau}^{\top}, \boldsymbol{\xi}_{\tau}^{\top}, \log \boldsymbol{\phi}_{\tau}^{\top})^{\top} \in \mathbb{R}^{p+m+1}$ denote the parameter of interest, where $\boldsymbol{\xi}_{\tau}$ is an unrestricted m -dimensional vector, $1 \leq m \leq q(q+1)/2$, of non-redundant parameters in $\boldsymbol{\Sigma}_{\tau}$ (e.g., see Pinheiro and Bates, 1996) and $\boldsymbol{\phi}_{\tau} = (\phi_{\tau,1}, \phi_{\tau,2}, \dots, \phi_{\tau,s})^{\top}$. Our goal is to maximize the marginal log-likelihood

$$\begin{aligned} \ell(\boldsymbol{\theta}_{\tau}; \mathbf{y}) &= N \log \left\{ \frac{\tau(1-\tau)}{\sigma_{\tau}} \right\} - \frac{M}{2} \log |\tilde{\boldsymbol{\Sigma}}_{\tau}| - \frac{1}{2} \log |\tilde{\boldsymbol{\Phi}}_{\tau}| \\ &+ \log \int_{\mathbb{R}^H} \left\{ \prod_{i=1}^M \int_{\mathbb{R}^q} \frac{\exp \left[-\left\{ 2\rho_{\tau} (\mathbf{y}_i - \mathbf{F}_i \boldsymbol{\beta}_{\tau} - \mathbf{Z}_i \mathbf{u}_{\tau,i} - \mathbf{B}_i \mathbf{v}_{\tau}) + \mathbf{u}_{\tau,i}^{\top} \tilde{\boldsymbol{\Sigma}}_{\tau}^{-1} \mathbf{u}_{\tau,i} \right\} / 2\sigma_{\tau} \right] / (2\pi\sigma_{\tau})^{q/2}}{(2\pi\sigma_{\tau})^{q/2}} d\mathbf{u}_{\tau,i} \right\} \\ &\times \frac{\exp \left(-\frac{1}{2\sigma_{\tau}} \mathbf{v}_{\tau}^{\top} \tilde{\boldsymbol{\Phi}}_{\tau}^{-1} \mathbf{v}_{\tau} \right)}{(2\pi\sigma_{\tau})^{H/2}}, \end{aligned} \quad (5)$$

where $\tilde{\boldsymbol{\Sigma}}_{\tau} = \boldsymbol{\Sigma}_{\tau}/\sigma_{\tau}$ and $\tilde{\boldsymbol{\Phi}}_{\tau} = \boldsymbol{\Phi}_{\tau}/\sigma_{\tau}$ are the scaled variance-covariance matrices of the random effects. Note that this is a three-level hierarchical model, with the innermost grouping factor represented by the clusters i and the outermost factor represented by one single-level group (i.e., the entire sample). Despite the three levels, we define $\hat{Q}_{\mathbf{y}_i | \mathbf{u}_i=0, \mathbf{x}_i, \mathbf{z}_i}^{(0)}(\tau) = \mathbf{F}_i \hat{\boldsymbol{\beta}}_{\tau} + \mathbf{B}_i \hat{\mathbf{v}}_{\tau}$ as the predictions at level 0 since the smooth terms originally 'belong' to the fixed design matrix.

Similarly, we define $\hat{Q}_{\mathbf{y}_i|\mathbf{u}_i, \mathbf{x}_i, \mathbf{z}_i}^{(1)}(\tau) = \mathbf{F}_i \hat{\boldsymbol{\beta}}_\tau + \mathbf{Z}_i \hat{\mathbf{u}}_{\tau,i} + \mathbf{B}_i \hat{\mathbf{v}}_\tau$ as the predictions at level 1 (i.e., at the cluster level).

Estimation proceeds using a double approximation:

1. the loss function $\rho_\tau(r)$ is first smoothed at the kink $r = 0$;
2. the integral in (5) is then solved using a Laplacian approximation for the (smoothed) loss function.

As proposed by [Geraci \(2017a\)](#), we consider the following smooth approximation ([Madsen and Nielsen, 1993](#); [Chen, 2007](#)):

$$\kappa_{\omega,\tau}(r) = \begin{cases} r(\tau-1) - \frac{1}{2}(\tau-1)^2\omega & \text{if } r \leq (\tau-1)\omega, \\ \frac{1}{2\omega}r^2 & \text{if } (\tau-1)\omega \leq r \leq \tau\omega, \\ r\tau - \frac{1}{2}\tau^2\omega & \text{if } r \geq \tau\omega, \end{cases} \quad (6)$$

where $r \in \mathbb{R}$ and $\omega > 0$ is a scalar ‘‘tuning’’ parameter. A similar approximation is given by [Muggeo, Sciandra and Augugliaro \(2012\)](#) who claimed that their method provides a better approximation than [Chen’s \(2007\)](#) algorithm. However, no analytical evidence was provided in their paper to support such a claim. This point might offer scope for additional investigation but, here, it represents a secondary issue and will not be discussed any further.

We then replace the function ρ_τ in (5) with $\kappa_{\omega,\tau}$ to obtain a smoothed likelihood and apply a second-order Taylor expansion ([Pinheiro and Chao, 2006](#)) to the resulting exponent. After some algebra, we obtain the following Laplacian approximation

$$\ell_{\text{LA}}(\boldsymbol{\theta}_\tau; \mathbf{y}, \hat{\mathbf{w}}_\tau) = N \log \left\{ \frac{\tau(1-\tau)}{\sigma_\tau} \right\} - \frac{1}{2} \left(\log |\tilde{\boldsymbol{\Psi}}_\tau \ddot{\mathbf{H}}| + \sigma_\tau^{-1} h_0 \right),$$

where $\tilde{\boldsymbol{\Psi}}$ is the scaled variance-covariance matrix of $\mathbf{w}_\tau = (\mathbf{u}_\tau^\top, \mathbf{v}_\tau^\top)^\top$, and h_0 and $\ddot{\mathbf{H}}$ are the terms of order, respectively, 0 and 2 of the above-mentioned Taylor expansion around the mode $\hat{\mathbf{w}}_\tau$ (see Appendix A for more details).

When using the asymmetric Laplace as pseudo-likelihood, inference should be confined to point estimation (see for example [Yang, Wang and He, 2016](#)). Standard errors of non-random parameters estimates can be calculated using block bootstrap ([Efron and Tibshirani, 1998](#)), although this increases the computational cost. Bootstrap confidence intervals have been shown to have good coverage in LQMMs ([Geraci and Bottai, 2014](#)). Given the relatively large size of the MCS dataset, for the analysis in Section 6 we implemented an adaptation of the method by [Kleiner et al. \(2014\)](#). The general idea is to perform a bootstrap on several subsets of the original data and then summarize measures of uncertainty from all subsets. This strategy, called ‘‘bag of little bootstraps’’ (BLB), greatly reduces the computing cost when the sample size is large (see [Kleiner et al., 2012, 2014](#), for more details). The original method was developed for IID observations. Since we are dealing with clusters, we adapted the BLB approach as follows:

1. sample without replacement s subsets of size $b < M$ from the pool of M clusters (random partition);
2. for each of the s subset, repeatedly (R times) take a bootstrap sample of size M and fit an AQMM for each replicate;
3. for each of the s subsets, calculate the bootstrap variance;
4. as final estimate of the standard error, take the square root of the average of the s variances in step 3.

As explained by the authors, the advantage of the BLB approach as compared to traditional bootstrap lies in the smaller size of the subsets. Although the nominal bootstrap sample size is M , there are at most b unique clusters in each subset. To obtain a bootstrap replicate, we only need a sample from a multinomial distribution with M trials and uniform probability over b possible events. Estimation proceeds with a weighted likelihood, where the cluster-specific weights are given by the multinomial counts.

4.4. Implementation

The methods described in this section were implemented as an add-on to the R package `1qmm` (Geraci, 2014). The add-on is currently available from the author's website (<https://marcogeraci.wordpress.com>) and will appear in a future release of the main package. The core function made use of routines available from the `mgcv` (Wood, 2006a) and `nlme` (Pinheiro et al., 2017) packages using syntax and options (e.g., selection of spline models) that are familiar to the users of these packages.

5. Simulation study

We ran a simulation study to assess the proposed methods. In our analysis, we considered the two most relevant alternatives for additive regression modelling. The first is based on additive mixed-effects regression (AMM), which is available in the R package `mgcv`. This package makes use of `nlme`'s fitting routines. The other is represented by Fenske et al.'s (2013) additive fixed-effects quantile regression (AFEQR) for longitudinal data, which is available in the `mboost` package (Hofner et al., 2014). Since the former approach aims at modelling the conditional expectation of the outcome under the assumption of normal errors, AQMM should have an advantage over AMM when the true errors are non-normal and the location-shift hypothesis of the normal model is violated. On the other hand, AFEQR is directly comparable to AQMM since they both aim at the conditional quantiles of the outcome with no assumption about the error distribution. However, as noted in Section 3.1, there are two basic differences between these two quantile regression approaches since in AQMM: (i) the cluster-specific effects are assumed to be random as opposed to fixed, thus a covariance structure between effects can be introduced; and (ii) the level of smoothing of the nonparametric terms is automatically estimated from the data (as reciprocal of the variance components) as opposed to prior specification. These are

not necessarily advantages (or disadvantages) but they do represent aspects to consider when choosing a strategy for modelling and estimation.

The data were generated according to the following model

$$y_{ij} = \beta_0 + \beta_1 \sin(x_{ij,1}) + \frac{\beta_2}{1 + \exp\{-(x_{ij,2} - 0.5)/0.1\}} \\ + \beta_3 x_{ij,3} + \beta_4 x_{ij,4} + \mathbf{z}_{ij}^\top \mathbf{u} + (1 + \gamma x_{ij,3})\epsilon, \quad j = 1, \dots, n \quad i = 1, \dots, M \quad (7)$$

where $\beta = (1, 4, 15, 4, 3)^\top$, $x_{ij,1} \sim \mathcal{U}(0, 4\pi)$, $x_{ij,2} \sim \mathcal{U}(0, 1)$, $x_{ij,3} \sim \text{Bin}(1, 0.3)$, $x_{ij,4} \sim \mathcal{N}(0, 1)$, $\mathbf{z}_{ij} = (1, x_{ij,4})^\top$, $\mathbf{u} \sim \mathcal{N}(\mathbf{0}, \Sigma)$, and

$$\Sigma = \begin{pmatrix} 2 & 0.8 \\ 0.8 & 1 \end{pmatrix}.$$

In one scenario, we set $\gamma = 0$ (homoscedastic), while in a separate scenario we set $\gamma = 1$ (heteroscedastic). Within these two scenarios, the error was generated according to either a standard normal, a Student's t -distribution with 3 degrees of freedom, or a χ^2 -distribution with 3 degrees of freedom. Thus, in total there were $2 \times 3 = 6$ different models. For each model, a balanced dataset was generated according to 6 sample size combinations of $n \in \{5, 10\}$ and $M \in \{50, 100, 500\}$, yielding $6 \times 6 = 36$ simulation cases. Each case was replicated $R = 500$ times.

For each replication, we fitted the AQMM defined in (2) for $\tau \in \{0.1, 0.5, 0.95\}$ using a cubic spline for the nonlinear terms associated with $x_{ij,1}$ and $x_{ij,2}$. The model also included a random intercept and a random slope for $x_{ij,4}$ with a symmetric positive-definite covariance matrix. We followed the estimation algorithm described in Appendix A. We used a Nelder-Mead algorithm to maximize the approximated log-likelihood and a tolerance of 10^{-5} for the relative change of the log-likelihood as the stopping criterion. The modal random effects (A.7) were estimated using a Broyden-Fletcher-Goldfarb-Shanno (BFGS) algorithm with gradient calculated as in (A.5). Since different strategies can be used to determine the starting values, we considered a naïve and a model-based approach. In the former case, we used the least squares (LS) estimate for β_τ , the identity matrix for Σ_τ , the mean of the absolute LS residuals for σ_τ , and half the standard deviation of y for ω . The random effects were all set equal to 0. In the latter case, we used parameter and random effects estimates from an AMM. All the results reported in this paper refer to the latter approach since it gave a superior performance.

The AFEQR models were fitted following Fenske et al.'s (2013) recommendations for the settings of the boosting algorithm, namely the maximum number of boosting iterations, the step length parameter $\nu \in (0, 1]$, and the degrees of freedom of the base-learners. The first two parameters were set to 5000 and 0.1, respectively, as determined by cross-validation (separately for the homoscedastic and the heteroscedastic scenarios). As explained by the authors, these two 'hyper-parameters' control the shrinkage of the estimates. The larger the step

length (or the smaller the number of iterations), the more biased and shrunk to zero the estimates will be. The number of degrees of freedom was set to 3 for each term of the boosting algorithm. Since the degree of smoothing is controlled by the number of boosting iterations, the final degree of smoothing at the end of the algorithm can still reach a higher order than that imposed by the initial degrees of freedom (Fenske et al., 2013). We used the `mboost` package (v. 2.8-1) in the R environment for statistical computing and graphics (R Core Team, 2014) (v. 3.4.2) on a desktop computer with a 3.60GHz quad core i7-4790 processor and 32 gigabytes of RAM.

As a measure of performance, we calculated the bias and the root mean squared error (RMSE) of the level-1 predicted quantile functions. The RMSE of the predictions is given by

$$\frac{1}{N} \sum_{i=1}^M \sum_{j=1}^n \left\{ \hat{Q}_{y_{ij}}^{(1)}(\tau) - Q_{y_{ij}}(\tau) \right\}^2,$$

where $Q_{y_{ij}}(\tau)$ denotes the true τ th conditional quantile function based on model (7). Analogously, we calculated the *relative* bias and RMSE of the coefficients for the linear terms, namely β_3 and β_4 . Note that these coefficients do not vary across quantiles in the homoscedastic scenario. In contrast, the value of the coefficient for $x_{ij,3}$ depends on τ in the heteroscedastic scenario. Its ‘true’ value was determined empirically by fitting a linear quantile regression model (Koenker and Bassett, 1978) with 4th degree polynomials on the nonlinear terms for 10,000 samples of size 5,000. Finally, we determined the proportion of negative residuals (PNR)

$$\frac{1}{N} \sum_{i=1}^M \sum_{j=1}^n I \left\{ y_{ij} - \hat{Q}_{y_{ij}}^{(1)}(\tau) < 0 \right\},$$

which is expected to be approximately equal to τ . All summary measures were averaged over the replications.

Given the large number of results of the simulation study, all the tables are reported in Appendix B and the results are summarized here as follows.

1. Prediction of conditional quantiles:

Homoscedastic scenario AQMM showed bias and RMSE lower than those of AFEQR consistently across all sample sizes for $\tau \in \{0.1, 0.95\}$. At the median, AQMM and AFEQR gave similar results, both showing low bias and RMSE values. The RMSE of AMM was particularly large in the case with asymmetric errors, as one would expect. However, in the case with normal errors, it was comparable to that of AQMM and surprisingly larger than that of AFEQR. Across quantiles, PNR rates for AQMM (and AFEQR) were equal to the expected nominal τ or differed at most by one hundredth.

Heteroscedastic scenario AQMM still had a clear advantage over AFEQR except at the median, where again the two performed similarly, and

at $\tau = 0.95$ under skewed errors. The performance of AMM relative to AQMM or AFEQR was comparable to that seen in the homoscedastic scenario.

2. Estimation of β_3 :

Homoscedastic scenario AQMM performed well as compared to AFEQR in terms of both bias and RMSE consistently across all quantiles and sample sizes. In particular, the bias of AQMM was much below 1% for the most part. In contrast, AFEQR's bias ranged from 4% to 15% and was more severe on the tails. At the median, AMM's performance was comparable to that of AQMM in terms of bias, but it was otherwise inferior in terms of RMSE.

Heteroscedastic scenario As compared to the homoscedastic scenario, AQMM and AFEQR showed larger biases on the tails, with percentages ranging from below 1% to 6% and from 7% to 20%, respectively. AQMM had, as before, consistently lower bias than AFEQR as well as lower RMSE, though the latter was occasionally higher for AQMM at lower sample sizes. At the median, the performance of AMM in terms of bias was rather poor under the scenario with skewed errors, but reasonable under the two scenarios with symmetric errors. In contrast, AMM was less efficient than AQMM in all three error scenarios at all sample sizes.

3. Estimation of β_4 :

Homoscedastic scenario AQMM outperformed AFEQR in terms of both bias and RMSE consistently across all sample sizes for $\tau \in \{0.1, 0.5\}$. AFEQR's bias was, again, particularly high and around 15% at $\tau = 0.1$. At $\tau = 0.95$, the bias of AQMM was larger than that seen for β_3 and somewhat erratic in the case with asymmetric errors, presumably due to the fact that the random component of the model includes x_4 and thus the estimation of β_4 is affected by the Laplacian approximation. In contrast, AFEQR gave larger RMSE values than AQMM but, occasionally, lower biases. At the median, AMM performed well in terms of bias in all scenarios but was less efficient than AQMM.

Heteroscedastic scenario The results were similar to those obtained in the heteroscedastic scenario.

Finally, we provide a brief report on the computational performance and the sensitivity of the results to different starting values. AQMM reached convergence in 98.2% of the replications. The median number of iterations to reach convergence for one model was 19 (min 5, max 293), while the median of the smoothing parameter ω at the last iteration was approximately 7.1×10^{-5} (min 4.0×10^{-84} , max 1.1×10^{-2}).

When using the naïve approach to determine the starting values for AQMM, the estimation algorithm converged 100% of the times, and took on average less iterations and a shorter time to converge. The median number of iterations to

reach convergence for one model was 13 (min 3, max 20), while the median of the smoothing parameter ω at the last iteration was approximately 4.0×10^{-4} (min 4.1×10^{-6} , max 4.9×10^{-1}). However, the bias and RMSE were in general slightly higher than those reported in Supplementary Materials. Regardless, the conclusions reached about the performance of AQMM relative to AFEQR and AMM were the same as those discussed above.

6. Data analysis

The MCS accelerometer data were collected between May 2008 and August 2009 from participating children of the fourth sweep of the parent longitudinal survey, which provided information on several covariates, including socio-demographic and behavioural variables. A number of cleaning and processing procedures were applied to the raw accelerometer data (Geraci et al., 2012; Rich et al., 2014) using the R package `pawacc` (Geraci, 2017b). Out of 12,625 children participating in the study, approximately 6,500 provided reliable data, the latter defined as data from accelerometers that were deemed to have been worn for at least two days, at least 10 hours each day (Rich et al., 2013; Griffiths et al., 2013b). However, for the purpose of our analysis, we retained observations only for those children with reliable data between 7:00 and 20:00 of each day of the week.

We considered several covariates. Linear terms pertaining to the socio-demographic domain were sex (binary, reference: male) and ethnic group (binary, reference: white) of the child, and OECD equivalized income quintiles (categorical, reference: fifth quintile). Linear terms pertaining to the behavioural domain were time spent reading for enjoyment (binary, reference: often), mode of transport to/from school (binary, reference: active), number of cars or vans owned (categorical, reference: two). Linear terms pertaining to the temporal domain were day of the week (binary, reference: weekday) and calendar season (categorical, reference: summer). Finally, we considered three nonparametric terms, one for time of the day on weekdays, one for time of the day on weekends, and one for body mass index (BMI). The outcome variable was accelerometer counts. The analysis was restricted to singletons born in England. This decision was motivated by the ethnic composition of the sample, consisting of almost all white children in Wales, Scotland and Northern Ireland. Since ethnicity is a strong predictor of physical activity (Griffiths et al., 2013a) and ethnicity is confounded with country, we removed children from Celtic countries. Further, we excluded 15 children with missing information on ethnicity and BMI. A summary of the dataset is given in Table 1. Our sample comprised 1,154 children for whom accelerometer counts were aggregated over 10-minute intervals between 7:00 and 20:00 (thus producing 79 time points), for seven days of the week. In total, this gave $N = 638,162$ accelerometer measurements (that is, $n_i = 79 \times 7$, $i = 1, \dots, 1154$).

Using a similar notation as in (2), the τ th additive linear quantile regression

TABLE 1
Categorical and continuous variables for English children of the Millennium Cohort Study.
The dataset consists of 638,162 accelerometer measurements, aggregated over 10-minute intervals, from a total of 1154 children. Note that the reference categories are the modal categories.

Variable	Levels	Children (%)	Measurements (%)
Sex	Male (reference) Female	614 (53.2) 540 (46.8)	
Ethnicity	White (reference) Other than white ^a	962 (83.4) 192 (16.6)	
Income quintile	1 2 3 4 5 (reference) Often (reference) Not often ^b	117 (10.1) 170 (14.7) 220 (19.1) 318 (27.6) 329 (28.5) 998 (86.5) 156 (13.5)	
Reading for pleasure	Active (reference) Passive	604 (52.3) 550 (47.7)	
Transportation to/from school	0 1 2 (reference) 3 or more	65 (5.6) 412 (35.7) 620 (53.7) 57 (5.0)	
Number of cars or vans owned	Monday through Friday (reference) Saturday or Sunday		455,830 (71.4) 182,332 (28.6)
Day of the week	Autumn Winter Spring Summer (reference)		230,285 (36.1) 13,509 (2.1) 82,634 (12.9) 311,734 (48.9)
Season			
Variable	Unit	FNS ^c	
Time of the day	min	—	
BMI	kg/m ²	(11.2, 15.1, 16.1, 17.5, 32.6)	
Accelerometer counts (×1000)	—	(0, 0.9, 3.1, 7.5, 297.1)	

^a Mixed ethnicity, Indian, Pakistani, Bangladeshi, and Black.

^b Less than once or twice a week.

^c Five-number-summary: minimum, three quartiles, and maximum.

model was specified as

$$\begin{aligned}
Q_{y_{ij}|\mathbf{u}_i, \mathbf{x}_i, \mathbf{z}_i}^*(\tau) = & \beta_{\tau,0} + \sum_{h=1}^{H_1} v_{\tau,1} B_h^{(1)}(t_{j,0}) + \sum_{h=1}^{H_2} v_{\tau,2} B_h^{(2)}(t_{j,1}) + \sum_{h=1}^{H_3} v_{\tau,3} B_h^{(3)}(\text{BMI}_i) \\
& + \beta_{\tau,1} \text{sex}_{i,1} + \beta_{\tau,2} \text{ethnicity}_{i,1} + \beta_{\tau,3} \text{income}_{i,1} + \beta_{\tau,4} \text{income}_{i,2} + \\
& + \beta_{\tau,5} \text{income}_{i,3} + \beta_{\tau,6} \text{income}_{i,4} + \beta_{\tau,7} \text{reading}_{i,1} + \beta_{\tau,8} \text{transport}_{i,1} \\
& + \beta_{\tau,9} \text{cars}_{i,0} + \beta_{\tau,10} \text{cars}_{i,1} + \beta_{\tau,11} \text{cars}_{i,3} + \beta_{\tau,12} \text{weekend}_{i,1} \\
& + \beta_{\tau,13} \text{autumn}_i + \beta_{\tau,14} \text{winter}_i + \beta_{\tau,15} \text{spring}_i + \mathbf{z}_{ij}^\top \mathbf{u}_{\tau,i}, \quad (8)
\end{aligned}$$

for $\tau \in \{0.1, 0.5, 0.9, 0.95, 0.99\}$. For fitting purposes, the outcome was scaled by 10^4 . The variables $t_{j,0}$ and $t_{j,1}$, $j = 1, \dots, 79$, denote the time of the day for, respectively, weekdays and weekend days. Time was expressed as minutes divided by 60×24 (e.g., with 0.29 corresponding to 7:00 and 0.83 to 20:00) and then centered about its mid-value (0.56 corresponding to 13:30). Similarly, BMI was centered about its mode (15.5 kg/m^2). Given the large size of the dataset, smooth terms were modelled using low-rank thin plate splines (Wood, 2003), which have been shown to possess optimal properties both statistically and computationally. The random effects $\mathbf{u}_i = (u_{i,0}, u_{i,1}, u_{i,t_0}, u_{i,t_1})^\top$ were assumed to follow a multivariate normal distribution with symmetric positive-definite variance-covariance matrix

$$\boldsymbol{\Sigma} = \begin{bmatrix} \sigma_0^2 & \sigma_{0,1} & \sigma_{0,t_0} & \sigma_{0,t_1} \\ \sigma_1^2 & \sigma_{1,1} & \sigma_{1,t_0} & \sigma_{1,t_1} \\ \sigma_{t_0}^2 & \sigma_{t_0,1} & \sigma_{t_0,t_1} & \sigma_{t_1}^2 \end{bmatrix}.$$

The first two terms of (8) can be interpreted as the τ th time-specific quantile function of accelerometer counts on an summer weekday for a boy of white ethnicity with modal BMI living in a household in the highest income quintile and with two cars, who reads often (at least once or twice a week) and walks or bikes from/to school (as opposed to moving by car or bus), and whose temporal (linear) trajectory belongs to the zero (or modal) random-effect cluster.

We made an attempt to fit an analogous AMM to obtain starting values for AQMM. However, the function `gamm` failed due to insufficient memory. We also tried with a smaller subset of 200 children, but the `gamm` function failed with a convergence error. Given the satisfactory simulation results, we therefore used the naïve approach described in Section 5 to determine the starting values.

The plot in Figure 2 shows the estimated quantile function at level 0 for a child in the reference group. Diurnal patterns show markedly different shapes during the week. On weekdays, there are multiple peaks of activity in the morning and early afternoon, followed by a plateau of higher activity in the evening. On weekends, the trajectories look flatter and are characterized by two grand peaks around 11:00 and 17:00.

Estimates of the fixed effects and standard errors from AQMM are reported in Table 2. The latter were obtained using the BLB approach described in Section 4.3 with a fivefold partition ($b \approx 230$) and $R = 50$ bootstrap replications.

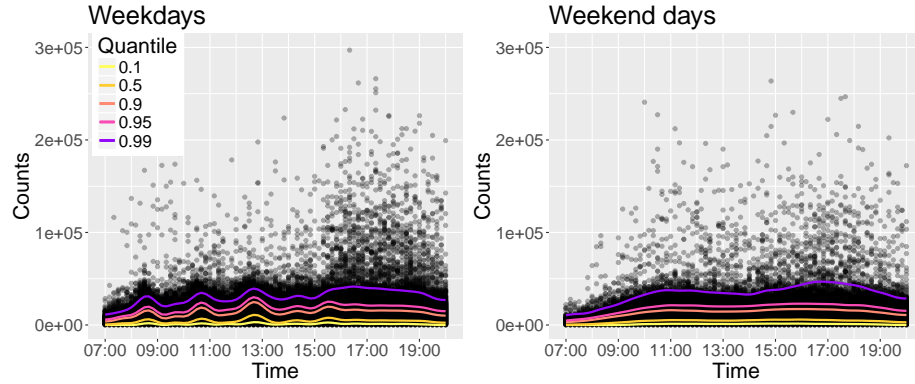


FIGURE 2. Accelerometer counts observed between 7:00 and 20:00 and aggregated over 10-minute intervals in 1154 English children of the UK Millennium Cohort Study, by days of the week (Monday through Friday, weekdays; Saturday and Sunday, weekend). Solid lines represent conditional quantile functions estimated for a child in the reference group for 5 quantile levels (0.1, 0.5, 0.9, 0.95, 0.99).

Some of the findings are consistent with those from previous analyses (Griffiths et al., 2013a; Sera et al., 2017) that focused on the central part of the distribution, namely: girls and children of ethnicity other than white are less active than their peers; reading frequently during the week is negatively associated with activity; and higher activity levels characterize spring and summer, followed by autumn and winter.

However, the narrative emerging from Table 2 is more variegated than this. First of all, there is a gradient across quantiles of increasingly larger differences in activity levels for girls and children of ethnicity other than white. Secondly, activity is lower in children from less affluent households at the most extreme quantile. In particular, activity is lower in those from economically disadvantaged (first quintile) across all quantiles. However, the estimates of the coefficients for income have large standard errors, resulting in statistical non-significance at the 95% level. The effects associated with reading and mode of transportation does not seem to be important, neither practically nor statistically. In contrast, there are marked differences between children living in households with two vehicles (reference) and those with none, the latter being substantially more active. It also seems that at the quantile 0.99, there is a *U*-shaped relationship between car/van ownership and activity counts.

While main effects of weekend on activity levels are approximately the same as those during the rest of the week across several quantiles, there is a rather strong positive weekend effect at the more extreme quantile. The results reported by Sera et al. (2017) showed no weekend effect, which is likely the consequence of averaging out stronger and weaker effects. Finally, it is interesting to note that the magnitude of the seasonal effects too increases with increasing quantiles. This is consistent with another quantile regression analysis of the MCS accelerometer

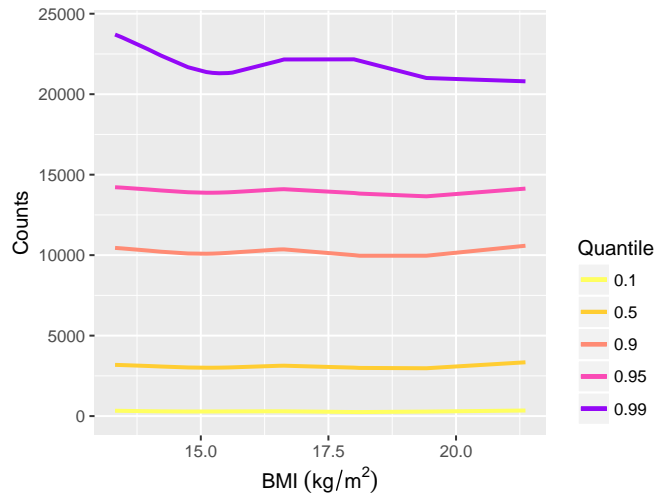


FIGURE 3. Smooth functions of body mass index (BMI) estimated for a child in the reference group of the UK Millennium Cohort Study physical activity dataset for 5 quantile levels (0.1, 0.5, 0.9, 0.95, 0.99).

data (Geraci and Farcomeni, 2016).

The estimated effect of BMI on activity counts for a child in the reference group is depicted in Figure 3. While the relationship is roughly constant up to the quantile 0.95, it is nonlinear at $\tau = 0.99$, with an overall negative gradient. The variance of the corresponding smooth term (Table 2) indicates a stronger penalty on the spline coefficients at the most extreme quantile.

The estimated standard deviations of the random effects show larger variability of individual linear trends (intercepts and temporal slopes) at the median and at $\tau = 0.99$ (Table 2). The correlation between random effects within weekdays or within weekends is strong, but the cross-correlation between weekdays and weekends terms is substantially weaker in the second half of the conditional distribution. This means that children tend to have trends of higher-intensity activity that are less similar between weekdays and weekends.

Individual trajectories of accelerometer counts for two children of the MCS are plotted in Figure 4. Despite both being white females with similar BMI (~ 15.6), living in a household with income in the lowest quintile and one car, having similar behaviors in terms of reading (often) and transportation (passive), they showed somewhat different daily patterns during summer weekend days. In particular, the conditional distribution was markedly skewed for the girl with identifier M16179P.

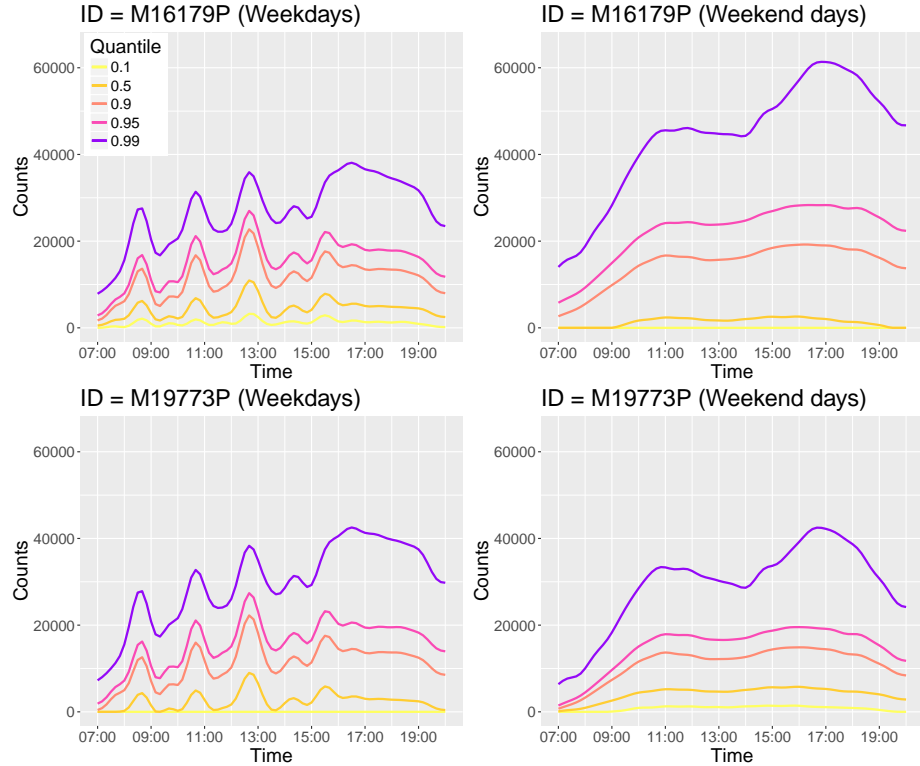


FIGURE 4. Cluster-specific conditional quantile functions for two children (labelled M16179P and M19773P) of the UK Millennium Cohort Study physical activity dataset for 5 quantile levels (0.1, 0.5, 0.9, 0.95, 0.99), by days of the week (Monday through Friday, weekdays; Saturday and Sunday, weekend).

7. Conclusion

We have developed a novel additive model for quantile regression when data are clustered. As compared to alternative approaches, ours has unique features, namely the mixed-effects representation of smoothing splines, which in turn leads to automatic smoothing selection, and the ability to model the variance-covariance matrix of the random effects.

As shown in a simulation study, the performance of AQMM was satisfactory despite the minimal tuning of the estimation algorithm. This takes a little burden away from the user who may instead focus their attention on other aspects of the analysis. This can be an asset if the data presents complexities as those illustrated in the MCS accelerometer analysis. In particular, the presence of a large number of regression coefficients and multiple smooth terms hinders the application of computationally intensive smoothing selection (e.g., cross-validation) to large datasets.

Standard error calculation in AQMM is facilitated by bootstrap. We were able to overcome the relatively large size of the MCS dataset by using an adaptation of the BLB approach (Kleiner et al., 2014). However, the versatility of bootstrap comes at a (computational) price and its application is limited to more central quantiles unless the sample size (i.e., number of clusters) is adequate. Further research is needed to develop accurate ‘sampling-free’ approximations of standard errors in AQMM as well as in LQMM.

Finally, in contrast to estimation based on numerical quadrature (Geraci and Bottai, 2014), random effects estimates in AQMM are a by-product of the optimization algorithm rather than being calculated *post hoc*. However, the proposed algorithm can be more demanding in terms of computing time as compared to, say, numerical quadrature or boosting, with the computational bottleneck indeed represented by the estimation of the random effects. For example, it took about two hours to fit a single AQMM using the MCS dataset. While, on the one hand, the large size of this dataset impaired even one of the most refined software for linear mixed-effects models, on the other hand a possible improvement in computing speed of the proposed algorithm is conceivable and is part of future research.

Acknowledgements

This research has been supported by the National Institutes of Health – National Institute of Child Health and Human Development (Grant Number: 1R03HD084807-01A1). The co-operation of the participating Millennium Cohort families is gratefully acknowledged as is the contribution of the management team at the Centre for Longitudinal Studies, UCL Institute of Education to collecting and, together with the UK Data Archive and Economic and Social Data Service, making the data available.

TABLE 2

Estimated fixed effects (counts per 10 minutes) and, in brackets, their standard errors, followed by estimated standard deviations and correlations of the random effects, standard deviations of the random spline coefficients, and proportion of negative residuals (PNR) from the additive quantile mixed model for the Millennium Cohort Study physical activity data. The reference categories are given in Table 1.

Fixed effects	$\tau = 0.1$	$\tau = 0.5$	$\tau = 0.9$	$\tau = 0.95$	$\tau = 0.99$
Intercept	992 (101)	4408 (183)	13704 (305)	18473 (492)	31065 (1136)
Sex (female)	-24 (64)	-180 (95)	-2049 (222)	-2752 (328)	-3113 (843)
Ethnicity (not white)	-101 (104)	-82 (124)	-1126 (285)	-1696 (388)	-3964 (948)
Income quintile (1)	-43 (146)	-39 (216)	-483 (422)	-784 (567)	-2747 (1525)
Income quintile (2)	70 (124)	99 (148)	35 (337)	-2 (519)	-369 (1679)
Income quintile (3)	53 (95)	13 (129)	-237 (303)	-512 (448)	-1196 (1009)
Income quintile (4)	-44 (83)	35 (129)	-135 (273)	-56 (412)	776 (1089)
Reading for pleasure (not often)	92 (114)	122 (141)	8 (367)	69 (502)	-276 (1179)
Transportation (passive)	62 (72)	86 (87)	-274 (226)	-409 (363)	-209 (750)
Number of cars or vans (0)	25 (169)	-77 (224)	1121 (549)	1279 (581)	3315 (739)
Number of cars or vans (1)	53 (83)	75 (100)	564 (231)	682 (368)	2083 (850)
Number of cars or vans (3+)	4 (164)	-53 (224)	518 (496)	655 (809)	2586 (1072)
Day of the week (weekend)	-148 (103)	-131 (106)	-168 (223)	-45 (364)	3023 (1066)
Season (autumn)	12 (76)	-164 (91)	-958 (209)	-1067 (313)	-3155 (774)
Season (winter)	-3 (199)	-204 (326)	-1377 (561)	-1675 (705)	-2999 (1124)
Season (spring)	82 (117)	244 (156)	1242 (333)	2197 (528)	6027 (2224)
Linear basis term for time of the day (weekdays)	410 (50)	782 (33)	2050 (54)	2639 (107)	5374 (448)
Linear basis term for time of the day (weekend)	635 (56)	980 (46)	2620 (83)	3434 (158)	7659 (965)
Linear basis term for BMI	-40 (125)	-11 (51)	-16 (113)	-64 (166)	-95 (387)
Standard deviations (random effects)	$\tau = 0.1$	$\tau = 0.5$	$\tau = 0.9$	$\tau = 0.95$	$\tau = 0.99$
$\hat{\sigma}_0$ (intercept weekdays)	2969	3923	2882	2769	4897
$\hat{\sigma}_1$ (intercept weekend)	3015	3526	2842	2809	5054
$\hat{\sigma}_{t_0}$ (time of the day weekdays)	2868	3575	2817	2800	5069
$\hat{\sigma}_{t_1}$ (time of the day weekend)	2867	3376	2940	2858	5017
Correlations (random effects)	$\tau = 0.1$	$\tau = 0.5$	$\tau = 0.9$	$\tau = 0.95$	$\tau = 0.99$
$\hat{\rho}_{0,1}$	0.93	0.97	0.73	0.36	0.52
$\hat{\rho}_{0,t_0}$	0.99	0.99	0.94	0.89	0.93
$\hat{\rho}_{1,t_0}$	0.93	0.97	0.71	0.35	0.51
$\hat{\rho}_{0,t_1}$	0.93	0.97	0.73	0.37	0.52
$\hat{\rho}_{1,t_1}$	0.99	0.99	0.93	0.88	0.93
$\hat{\rho}_{t_0,t_1}$	0.93	0.97	0.72	0.36	0.51
Standard deviations (smooth terms)	$\tau = 0.1$	$\tau = 0.5$	$\tau = 0.9$	$\tau = 0.95$	$\tau = 0.99$
$\hat{\phi}_{\text{weekdays}}$	4136	15215	4114	4343	1722
$\hat{\phi}_{\text{weekend}}$	8385	14541	6699	2402	515
$\hat{\phi}_{\text{BMI}}$	2905	4945	7094	2777	181
PNR	0.11	0.50	0.90	0.95	0.99

Appendix A - Inference

The goal is to maximize the log-likelihood (5) with respect to the $(p+m+1) \times 1$ parameter vector $\boldsymbol{\theta}_\tau = (\boldsymbol{\beta}_\tau^\top, \boldsymbol{\xi}_\tau^\top, \log \boldsymbol{\phi}_\tau^\top)^\top$.

Let $\mathbf{r}_i = \mathbf{y}_i - \mathbf{F}_i \boldsymbol{\beta}_\tau - \mathbf{Z}_i \mathbf{u}_{\tau,i} - \mathbf{B}_i \mathbf{v}_\tau$ be the $n_i \times 1$ vector of residuals for the i th cluster with generic element r_{ij} , and define the corresponding sign vector $\mathbf{s}_i = (s_{i1}, \dots, s_{in_i})^\top$ with

$$s_{ij} = \begin{cases} -1 & \text{if } r_{ij} \leq (\tau - 1)\omega, \\ 0 & \text{if } (\tau - 1)\omega < r_{ij} < \tau\omega, \\ 1 & \text{if } r_{ij} \geq \tau\omega. \end{cases} \quad (\text{A.1})$$

(The notation above has been simplified since the r_{ij} 's as well as the s_{ij} 's should be written as functions of $\boldsymbol{\theta}_\tau$.) We apply the smooth approximation (Madsen and Nielsen, 1993; Chen, 2007) given in equation (6) to the elements of \mathbf{r}_i and write

$$\kappa_{\omega, \tau}(\mathbf{r}_i) \equiv \sum_{j=1}^{n_i} \kappa_{\omega, \tau}(r_{ij}) = \frac{1}{2} (\|\mathbf{r}_i\|_{\mathbf{A}_i}^2 + \mathbf{b}_i^\top \mathbf{r}_i + \mathbf{c}_i^\top \mathbf{1}_{n_i}), \quad (\text{A.2})$$

where \mathbf{A}_i is an $n_i \times n_i$ diagonal matrix with diagonal elements $\{\mathbf{A}_i\}_{jj} = (1 - s_{ij}^2)/\omega$, \mathbf{b}_i and \mathbf{c}_i are two $n_i \times 1$ vectors with elements

$$b_{ij} = s_{ij}((2\tau - 1)s_{ij} + 1)$$

and

$$c_{ij} = \frac{1}{2} \{(1 - 2\tau)\omega s_{ij} - (1 - 2\tau + 2\tau^2)\omega s_{ij}^2\},$$

respectively.

For a more compact notation, let $\mathbf{w}_\tau = (\mathbf{u}_\tau^\top, \mathbf{v}_\tau^\top)^\top$, $\mathbf{A} = \bigoplus_{i=1}^M \mathbf{A}_i$, $\mathbf{b} = (\mathbf{b}_1^\top, \dots, \mathbf{b}_M^\top)^\top$, $\mathbf{c} = (\mathbf{c}_1^\top, \dots, \mathbf{c}_M^\top)^\top$, $\mathbf{r} = (\mathbf{r}_1^\top, \dots, \mathbf{r}_M^\top)^\top$, $\mathbf{Z} = \bigoplus_{i=1}^M \mathbf{Z}_i$, $\mathbf{B} = [\mathbf{B}_1^\top \dots \mathbf{B}_M^\top]^\top$, $\mathbf{G} = [\mathbf{Z} \ \mathbf{B}]$, and $\tilde{\boldsymbol{\Psi}}_\tau = (\mathbf{I}_M \otimes \tilde{\boldsymbol{\Sigma}}) \oplus \tilde{\boldsymbol{\Phi}}$. We now define the function

$$\begin{aligned} h(\boldsymbol{\theta}_\tau, \mathbf{y}, \mathbf{u}_\tau, \mathbf{v}_\tau) &= \sum_{i=1}^M \left\{ \mathbf{r}_i^\top \mathbf{A}_i \mathbf{r}_i + \mathbf{b}_i^\top \mathbf{r}_i + \mathbf{c}_i^\top \mathbf{1}_{n_i} + \mathbf{u}_{\tau,i}^\top \tilde{\boldsymbol{\Sigma}}_\tau^{-1} \mathbf{u}_{\tau,i} \right\} + \mathbf{v}_\tau^\top \tilde{\boldsymbol{\Phi}}_\tau^{-1} \mathbf{v}_\tau \\ &= \mathbf{r}^\top \mathbf{A} \mathbf{r} + \mathbf{b}^\top \mathbf{r} + \mathbf{c}^\top \mathbf{1}_N + \mathbf{w}_\tau^\top \tilde{\boldsymbol{\Psi}}_\tau^{-1} \mathbf{w}_\tau. \end{aligned} \quad (\text{A.3})$$

The smoothed version of the log-likelihood (5) is then given by

$$\begin{aligned} \ell_S(\boldsymbol{\theta}_\tau; \mathbf{y}, \omega) &= N \log \left\{ \frac{\tau(1 - \tau)}{\sigma_\tau} \right\} - \frac{1}{2} \log |\tilde{\boldsymbol{\Psi}}_\tau| \\ &+ \log \int_{\mathbb{R}^{Mq+H}} \frac{\exp \left(-\frac{1}{2\sigma_\tau} h(\boldsymbol{\theta}_\tau, \mathbf{y}, \mathbf{u}_\tau, \mathbf{v}_\tau) \right)}{(2\pi\sigma_\tau)^{(Mq+H)/2}} d\mathbf{w}_\tau. \end{aligned} \quad (\text{A.4})$$

For $\omega \rightarrow 0$, we have that $\ell_S(\boldsymbol{\theta}_\tau; \mathbf{y}, \omega) \rightarrow \ell(\boldsymbol{\theta}_\tau; \mathbf{y})$.

Since h is differentiable with respect to \mathbf{w}_τ , we can derive the following quantities

$$\begin{aligned} \frac{\partial h(\boldsymbol{\theta}_\tau, \mathbf{y}, \mathbf{u}_\tau, \mathbf{v}_\tau)}{\partial \mathbf{u}_{\tau,i}} &= -\mathbf{Z}_i^\top (2\mathbf{A}_i \mathbf{r}_i + \mathbf{b}_i) + 2\tilde{\boldsymbol{\Sigma}}_\tau^{-1} \mathbf{u}_{\tau,i}, \\ \frac{\partial h(\boldsymbol{\theta}_\tau, \mathbf{y}, \mathbf{u}_\tau, \mathbf{v}_\tau)}{\partial \mathbf{v}_\tau} &= -\sum_{i=1}^M \{\mathbf{B}_i^\top (2\mathbf{A}_i \mathbf{r}_i + \mathbf{b}_i)\} + 2\tilde{\boldsymbol{\Phi}}_\tau^{-1} \mathbf{v}_\tau, \\ \frac{\partial^2 h(\boldsymbol{\theta}_\tau, \mathbf{y}, \mathbf{u}_\tau, \mathbf{v}_\tau)}{\partial \mathbf{u}_{\tau,i} \mathbf{u}_{\tau,i}^\top} &= 2 \left(\mathbf{Z}_i^\top \mathbf{A}_i \mathbf{Z}_i + \tilde{\boldsymbol{\Sigma}}_\tau^{-1} \right), \\ \frac{\partial^2 h(\boldsymbol{\theta}_\tau, \mathbf{y}, \mathbf{u}_\tau, \mathbf{v}_\tau)}{\partial \mathbf{v}_\tau \mathbf{v}_\tau^\top} &= \sum_{i=1}^M 2 \left(\mathbf{B}_i^\top \mathbf{A}_i \mathbf{B}_i \right) + 2\tilde{\boldsymbol{\Phi}}_\tau^{-1}, \\ \frac{\partial^2 h(\boldsymbol{\theta}_\tau, \mathbf{y}, \mathbf{u}_\tau, \mathbf{v}_\tau)}{\partial \mathbf{u}_{\tau,i} \mathbf{u}_{\tau,j}^\top} &= \mathbf{O}_{q \times q}, \quad i \neq j, \\ \frac{\partial^2 h(\boldsymbol{\theta}_\tau, \mathbf{y}, \mathbf{u}_\tau, \mathbf{v}_\tau)}{\partial \mathbf{v}_\tau \mathbf{u}_{\tau,i}^\top} &= 2\mathbf{B}_i^\top \mathbf{A}_i \mathbf{Z}_i. \end{aligned}$$

The above derivatives can be written more compactly for all clusters as

$$\frac{\partial h(\boldsymbol{\theta}_\tau, \mathbf{y}, \mathbf{u}_\tau, \mathbf{v}_\tau)}{\partial \mathbf{w}_\tau} = -\mathbf{G}^\top (2\mathbf{A}\mathbf{r} + \mathbf{b}) + 2\tilde{\boldsymbol{\Psi}}_\tau^{-1} \mathbf{w}_\tau, \quad (\text{A.5})$$

$$\frac{\partial^2 h(\boldsymbol{\theta}_\tau, \mathbf{y}, \mathbf{u}_\tau, \mathbf{v}_\tau)}{\partial \mathbf{w}_\tau \mathbf{w}_\tau^\top} = 2 \left(\mathbf{G}^\top \mathbf{A} \mathbf{G} + \tilde{\boldsymbol{\Psi}}_\tau^{-1} \right). \quad (\text{A.6})$$

Moreover, let

$$\hat{\mathbf{w}}_\tau \equiv (\hat{\mathbf{u}}_\tau, \hat{\mathbf{v}}_\tau) = \arg \min_{\mathbf{u}, \mathbf{v}} h(\boldsymbol{\theta}_\tau, \mathbf{y}, \mathbf{u}, \mathbf{v}) \quad (\text{A.7})$$

be the conditional mode of \mathbf{w}_τ . A second-order approximation of h around $\hat{\mathbf{w}}_\tau$ is given by

$$h(\boldsymbol{\theta}_\tau, \mathbf{y}, \mathbf{u}_\tau, \mathbf{v}_\tau) \simeq h_0 + \dot{\mathbf{h}}^\top (\mathbf{w}_\tau - \hat{\mathbf{w}}_\tau) + (\mathbf{w}_\tau - \hat{\mathbf{w}}_\tau)^\top \ddot{\mathbf{H}} (\mathbf{w}_\tau - \hat{\mathbf{w}}_\tau),$$

where $h_0 \equiv h(\boldsymbol{\theta}_\tau, \mathbf{y}, \hat{\mathbf{u}}_\tau, \hat{\mathbf{v}}_\tau)$, $\dot{\mathbf{h}} \equiv h'(\boldsymbol{\theta}_\tau, \mathbf{y}, \hat{\mathbf{u}}_\tau, \hat{\mathbf{v}}_\tau)$, and $\ddot{\mathbf{H}} \equiv h''(\boldsymbol{\theta}_\tau, \mathbf{y}, \hat{\mathbf{u}}_\tau, \hat{\mathbf{v}}_\tau)/2$. Since $\dot{\mathbf{h}}$ is zero at $\mathbf{w}_\tau = \hat{\mathbf{w}}_\tau$, we have finally the following Laplacian approximation of the (smoothed) log-likelihood (A.4)

$$\begin{aligned} \ell_{\text{LA}}(\boldsymbol{\theta}_\tau; \mathbf{y}, \hat{\mathbf{w}}_\tau) &= N \log \left\{ \frac{\tau(1-\tau)}{\sigma_\tau} \right\} - \frac{1}{2} \log |\tilde{\boldsymbol{\Psi}}_\tau| - \frac{1}{2\sigma_\tau} h_0 \\ &\quad + \log \int_{\mathbb{R}^{Mq+H}} (2\pi\sigma_\tau)^{-(Mq+H)/2} \exp \left\{ -\frac{1}{2\sigma_\tau} (\mathbf{w}_\tau - \hat{\mathbf{w}}_\tau)^\top \ddot{\mathbf{H}} (\mathbf{w}_\tau - \hat{\mathbf{w}}_\tau) \right\} d\mathbf{w}_\tau \\ &= N \log \left\{ \frac{\tau(1-\tau)}{\sigma_\tau} \right\} - \frac{1}{2} \left(\log |\tilde{\boldsymbol{\Psi}}_\tau \ddot{\mathbf{H}}| + \sigma_\tau^{-1} h_0 \right). \end{aligned} \quad (\text{A.8})$$

To maximize (A.8) with respect to $\boldsymbol{\theta}_\tau$, we can use a general purpose optimizer such the Nelder–Mead or the Broyden–Fletcher–Goldfarb–Shanno algorithms. For a given $\hat{\boldsymbol{\theta}}_\tau$, the scale σ_τ can be estimated from

$$\hat{\sigma}_\tau = (2N)^{-1} h_0. \quad (\text{A.9})$$

Note that (A.8) can be profiled with respect to σ_τ . Finally, for a given value of ω , the mode \mathbf{w}_τ can be obtained by means of Newton–Raphson (Pinheiro and Chao, 2006) using (A.5) and (A.6).

Estimation of the parameters can be carried out iteratively. The algorithm requires setting the starting value of $\boldsymbol{\theta}_\tau$ and σ_τ , the tuning parameter ω , the tolerance for the change in the log-likelihood, and the maximum number of iterations. Moreover, the modes of the random effects can be obtained by equating (A.5) to $\mathbf{0}$ and then solving for \mathbf{w}_τ . Specifically, this leads to the following system of equations

$$2\ddot{\mathbf{H}}\mathbf{w}_\tau = \mathbf{G}^\top \{2\mathbf{A}(\mathbf{y} - \mathbf{F}\boldsymbol{\beta}_\tau) + \mathbf{b}\}. \quad (\text{A.10})$$

Since the right-hand side depends on \mathbf{w}_τ through \mathbf{A} and \mathbf{b} , an estimate $\hat{\mathbf{w}}_\tau$ is obtained iteratively.

The pseudo-code of the complete algorithm is given below. This algorithm is based on a set of decreasing values of ω and has the appealing advantage of reducing the original non-smooth problem to an approximated L_2 problem.

SMOOTHING ALGORITHM WITH LAPLACIAN APPROXIMATION FOR
ADDITIVE QUANTILE MIXED MODELS

- (1) Set the maximum number of iterations T ; the factor $0 < \gamma < 1$ for reducing the tuning parameter ω ; the tolerance for the change in the log-likelihood; and $t = 0$. Estimate the starting values as follows:
 - (a) obtain an estimate for $\beta_\tau^{(0)}$ using an additive mixed model (AMM) (Wood, 2006b). If the AMM fitting algorithm fails, consider a standard linear least squares estimate of the fixed effects;
 - (b) obtain an estimate for $\xi_\tau^{(0)}$ and $\phi_\tau^{(0)}$ from the AMM fitted in step (a). If the AMM fitting algorithm fails, provide an arbitrary value;
 - (c) obtain an estimate for $\sigma_\tau^{(0)}$. For example, this can be estimated as the mean of the absolute residuals from step (1.a) above;
 - (d) provide a starting value $\omega^{(0)}$ (see, for example, Chen, 2007, p.143);
 - (e) using $\beta_\tau^{(0)}$, $\xi_\tau^{(0)}$, $\phi_\tau^{(0)}$, and $\sigma_\tau^{(0)}$, solve (A.7) to obtain $\mathbf{w}_\tau^{(0)}$ using an iterative method. See, for example, the R functions `optim` and `nlm`.
- (2) While $t < T$
 - (a) Update $\boldsymbol{\theta}_\tau^{(t)}$ by minimizing (A.8). See, for example, the R function `optim`.
 - (b) If the change in the log-likelihood is smaller than a given tolerance
 - (i) then return $\boldsymbol{\theta}_\tau^{(t+1)}$;
 - (ii) else set $\boldsymbol{\theta}_\tau^{(t+1)} = \boldsymbol{\theta}_\tau^{(t)}$; $\omega^{(t+1)} = \gamma \cdot \omega^{(t)}$; $t = t + 1$; go to step (2.a).
- (3) Update $\sigma_\tau^{(t)}$ and $\mathbf{w}_\tau^{(t)}$.

Appendix B - Simulation study results

B.1. Homoscedastic scenario

TABLE B1

Quantile 0.1 and homoscedastic scenario. Average bias and root mean squared error (RMSE) for $Q(0.1)$ from the additive quantile mixed model (AQMM) and the additive fixed-effects quantile regression (AFEQR). The expected proportion of negative residuals (PNR) is 0.1.

Sample size (n, M)	AQMM			AFEQR		
	PNR	Bias	RMSE	PNR	Bias	RMSE
<i>Normal</i>						
(5, 50)	0.11	0.27	1.69	0.10	-2.21	3.22
(10, 50)	0.10	0.12	1.71	0.10	-2.34	3.26
(5, 100)	0.10	0.26	1.69	0.10	-2.35	3.28
(10, 100)	0.10	0.11	1.69	0.10	-2.40	3.24
(5, 500)	0.10	0.23	1.67	0.10	-2.36	3.13
(10, 500)	0.10	0.13	1.69	0.10	-2.36	3.12
<i>Student's t</i>						
(5, 50)	0.10	0.01	1.65	0.10	-2.14	3.25
(10, 50)	0.10	-0.02	1.66	0.10	-2.25	3.25
(5, 100)	0.10	0.06	1.60	0.10	-2.29	3.29
(10, 100)	0.10	0.02	1.64	0.10	-2.32	3.23
(5, 500)	0.10	0.06	1.54	0.10	-2.29	3.10
(10, 500)	0.10	0.02	1.61	0.10	-2.29	3.10
<i>Chi-squared</i>						
(5, 50)	0.10	-0.01	1.56	0.10	-1.81	3.02
(10, 50)	0.09	-0.02	1.55	0.10	-1.94	3.01
(5, 100)	0.10	0.01	1.47	0.10	-1.98	3.06
(10, 100)	0.09	-0.01	1.54	0.10	-2.03	2.99
(5, 500)	0.10	0.04	1.40	0.10	-2.01	2.88
(10, 500)	0.10	0.03	1.51	0.10	-2.01	2.88

TABLE B2

Quantile 0.5 and homoscedastic scenario. Average bias and root mean squared error (RMSE) for $Q(0.5)$ from the additive quantile mixed model (AQMM), the additive fixed-effects quantile regression (AFEQR), and the additive mixed model (AMM). The expected proportion of negative residuals (PNR) is 0.5.

Sample size (n, M)	AQMM			AFEQR			AMM		
	PNR	Bias	RMSE	PNR	Bias	RMSE	PNR	Bias	RMSE
<i>Normal</i>									
(5, 50)	0.50	-0.00	1.66	0.50	-0.01	1.69	0.50	-0.00	1.65
(10, 50)	0.50	0.00	1.69	0.50	-0.02	1.50	0.50	-0.00	1.69
(5, 100)	0.50	0.01	1.66	0.50	0.00	1.50	0.50	0.01	1.66
(10, 100)	0.50	-0.00	1.68	0.50	-0.01	1.36	0.50	0.00	1.69
(5, 500)	0.50	0.00	1.65	0.50	-0.02	1.24	0.50	0.00	1.65
(10, 500)	0.50	0.00	1.69	0.50	-0.01	1.24	0.50	0.00	1.68
<i>Student's t</i>									
(5, 50)	0.50	-0.00	1.58	0.50	-0.00	1.79	0.50	-0.01	1.60
(10, 50)	0.50	-0.01	1.61	0.50	-0.03	1.57	0.50	-0.01	1.62
(5, 100)	0.50	0.00	1.56	0.50	-0.01	1.58	0.50	-0.00	1.57
(10, 100)	0.50	0.00	1.61	0.50	-0.01	1.43	0.50	0.00	1.62
(5, 500)	0.50	0.00	1.53	0.50	-0.01	1.30	0.50	0.00	1.53
(10, 500)	0.50	0.00	1.61	0.50	-0.02	1.30	0.50	0.00	1.61
<i>Chi-squared</i>									
(5, 50)	0.50	0.31	1.59	0.50	0.40	2.05	0.88	2.99	3.37
(10, 50)	0.50	0.24	1.59	0.50	0.37	1.80	0.87	3.01	3.39
(5, 100)	0.50	0.28	1.51	0.50	0.37	1.83	0.87	3.00	3.34
(10, 100)	0.50	0.19	1.55	0.50	0.33	1.64	0.86	3.00	3.37
(5, 500)	0.50	0.25	1.43	0.50	0.32	1.48	0.87	3.00	3.31
(10, 500)	0.50	0.18	1.52	0.50	0.33	1.47	0.86	3.00	3.36

TABLE B3

Quantile 0.95 and homoscedastic scenario. Average bias and root mean squared error (RMSE) for $Q(0.95)$ from the additive quantile mixed model (AQMM) and the additive fixed-effects quantile regression (AFEQR). The expected proportion of negative residuals (PNR) is 0.95.

Sample size (n, M)	AQMM			AFEQR		
	PNR	Bias	RMSE	PNR	Bias	RMSE
<i>Normal</i>						
(5, 50)	0.94	-0.33	1.72	0.95	3.03	4.01
(10, 50)	0.95	-0.16	1.72	0.95	3.22	4.12
(5, 100)	0.95	-0.29	1.70	0.95	3.27	4.17
(10, 100)	0.95	-0.15	1.70	0.95	3.32	4.17
(5, 500)	0.95	-0.28	1.68	0.95	3.30	4.08
(10, 500)	0.95	-0.15	1.70	0.95	3.30	4.08
<i>Student's t</i>						
(5, 50)	0.94	-0.16	1.76	0.95	2.74	3.86
(10, 50)	0.95	-0.09	1.73	0.95	2.90	3.92
(5, 100)	0.95	-0.19	1.68	0.95	2.96	3.97
(10, 100)	0.95	-0.11	1.68	0.95	3.02	3.96
(5, 500)	0.95	-0.19	1.57	0.95	2.99	3.85
(10, 500)	0.95	-0.11	1.63	0.95	2.99	3.85
<i>Chi-squared</i>						
(5, 50)	0.95	-0.70	2.18	0.95	1.49	3.36
(10, 50)	0.95	-0.43	2.01	0.95	1.79	3.37
(5, 100)	0.95	-0.68	1.97	0.95	1.82	3.39
(10, 100)	0.95	-0.44	1.86	0.95	1.91	3.33
(5, 500)	0.95	-0.65	1.67	0.95	1.86	3.15
(10, 500)	0.95	-0.43	1.65	0.95	1.86	3.12

TABLE B4

Quantile 0.1 and homoscedastic scenario. Average relative bias (%) and root mean squared error (RMSE) for β_3 from the additive quantile mixed model (AQMM) and the additive fixed-effects quantile regression (AFEQR).

Sample size (n, M)	AQMM Rel. bias	AQMM RMSE	AFEQR Rel. bias	AFEQR RMSE
<i>Normal</i>				
(5, 50)	-0.17	0.05	-6.05	0.43
(10, 50)	-0.22	0.03	-8.42	0.29
(5, 100)	0.02	0.03	-8.25	0.29
(10, 100)	0.20	0.01	-8.91	0.22
(5, 500)	-0.15	0.01	-9.23	0.17
(10, 500)	0.05	0.00	-9.14	0.15
<i>Student's t</i>				
(5, 50)	-0.54	0.17	-7.17	0.52
(10, 50)	0.01	0.07	-8.92	0.35
(5, 100)	-0.40	0.07	-9.23	0.38
(10, 100)	0.09	0.04	-8.98	0.24
(5, 500)	0.09	0.01	-9.51	0.19
(10, 500)	-0.06	0.01	-10.12	0.19
<i>Chi-squared</i>				
(5, 50)	-0.64	0.16	-7.81	0.50
(10, 50)	-0.21	0.06	-8.87	0.35
(5, 100)	-0.21	0.07	-9.49	0.36
(10, 100)	-0.01	0.03	-9.97	0.27
(5, 500)	0.20	0.01	-8.97	0.17
(10, 500)	-0.00	0.00	-9.94	0.18

TABLE B5

Quantile 0.5 and homoscedastic scenario. Average relative bias (%) and root mean squared error (RMSE) for β_3 from the additive quantile mixed model (AQMM), the additive fixed-effects quantile regression (AFEQR), and the additive mixed model (AMM).

Sample size (n, M)	AQMM		AFEQR		AMM	
	Rel. bias	RMSE	Rel. bias	RMSE	Rel. bias	RMSE
<i>Normal</i>						
(5, 50)	-0.50	0.04	-4.81	0.26	-0.53	0.13
(10, 50)	-0.13	0.02	-5.36	0.15	-0.10	0.09
(5, 100)	0.17	0.02	-4.70	0.14	0.16	0.10
(10, 100)	0.03	0.01	-4.70	0.08	0.02	0.06
(5, 500)	-0.11	0.00	-4.40	0.05	-0.11	0.04
(10, 500)	0.04	0.00	-4.59	0.04	0.00	0.03
<i>Student's t</i>						
(5, 50)	-0.37	0.08	-4.09	0.26	-0.20	0.22
(10, 50)	-0.00	0.03	-5.88	0.16	-0.25	0.14
(5, 100)	-0.20	0.03	-4.86	0.15	-0.51	0.15
(10, 100)	-0.05	0.01	-5.11	0.09	0.17	0.10
(5, 500)	-0.05	0.01	-4.57	0.05	-0.06	0.06
(10, 500)	-0.02	0.00	-4.98	0.05	-0.07	0.04
<i>Chi-squared</i>						
(5, 50)	0.07	0.15	-4.05	0.34	-0.07	0.30
(10, 50)	-0.24	0.08	-5.60	0.21	-0.45	0.21
(5, 100)	0.16	0.08	-5.22	0.18	-0.05	0.23
(10, 100)	-0.25	0.04	-5.45	0.13	-0.31	0.15
(5, 500)	0.23	0.02	-4.56	0.06	0.16	0.09
(10, 500)	-0.02	0.01	-4.65	0.05	-0.06	0.06

TABLE B6

Quantile 0.95 and homoscedastic scenario. Average relative bias (%) and root mean squared error (RMSE) for β_3 from the additive quantile mixed model (AQMM) and the additive fixed-effects quantile regression (AFEQR).

Sample size (n, M)	AQMM Rel. bias	AQMM RMSE	AFEQR Rel. bias	AFEQR RMSE
<i>Normal</i>				
(5, 50)	-1.15	0.07	-7.67	0.59
(10, 50)	-0.38	0.04	-7.08	0.33
(5, 100)	0.45	0.04	-7.66	0.36
(10, 100)	-0.07	0.02	-6.14	0.18
(5, 500)	-0.13	0.01	-5.54	0.10
(10, 500)	-0.07	0.00	-5.45	0.07
<i>Student's t</i>				
(5, 50)	0.86	0.33	-6.43	0.74
(10, 50)	-0.44	0.16	-7.31	0.37
(5, 100)	-0.03	0.13	-7.66	0.41
(10, 100)	0.54	0.08	-7.43	0.26
(5, 500)	-0.15	0.03	-6.35	0.13
(10, 500)	-0.41	0.02	-6.21	0.09
<i>Chi-squared</i>				
(5, 50)	-0.57	1.17	-14.98	1.55
(10, 50)	-0.75	0.67	-13.73	0.95
(5, 100)	0.50	0.70	-12.12	0.94
(10, 100)	0.39	0.37	-11.47	0.56
(5, 500)	0.29	0.14	-9.29	0.29
(10, 500)	-0.44	0.07	-8.98	0.20

TABLE B7

Quantile 0.1 and homoscedastic scenario. Average relative bias (%) and root mean squared error (RMSE) for β_4 from the additive quantile mixed model (AQMM) and the additive fixed-effects quantile regression (AFEQR).

Sample size (n, M)	AQMM Rel. bias	AQMM RMSE	AFEQR Rel. bias	AFEQR RMSE
<i>Normal</i>				
(5, 50)	0.59	0.03	-15.62	0.31
(10, 50)	0.40	0.03	-15.49	0.28
(5, 100)	0.60	0.02	-15.55	0.27
(10, 100)	0.37	0.02	-15.45	0.25
(5, 500)	0.85	0.00	-15.18	0.22
(10, 500)	0.28	0.00	-15.40	0.22
<i>Student's t</i>				
(5, 50)	1.70	0.06	-16.18	0.37
(10, 50)	0.60	0.03	-15.61	0.28
(5, 100)	1.38	0.03	-15.97	0.29
(10, 100)	0.04	0.02	-15.50	0.25
(5, 500)	1.52	0.01	-15.35	0.22
(10, 500)	0.55	0.00	-15.49	0.22
<i>Chi-squared</i>				
(5, 50)	2.13	0.08	-15.03	0.34
(10, 50)	0.53	0.03	-14.82	0.27
(5, 100)	1.63	0.03	-15.03	0.27
(10, 100)	0.43	0.02	-15.36	0.25
(5, 500)	1.27	0.01	-14.81	0.21
(10, 500)	0.40	0.00	-15.18	0.21

TABLE B8

Quantile 0.5 and homoscedastic scenario. Average relative bias (%) and root mean squared error (RMSE) for β_4 from the additive quantile mixed model (AQMM), the additive fixed-effects quantile regression (AFEQR), and the additive mixed model (AMM).

Sample size (n, M)	AQMM		AFEQR		AMM	
	Rel. bias	RMSE	Rel. bias	RMSE	Rel. bias	RMSE
<i>Normal</i>						
(5, 50)	-0.26	0.03	-5.64	0.09	-0.24	0.13
(10, 50)	-0.24	0.02	-6.61	0.08	-0.32	0.12
(5, 100)	-0.09	0.01	-5.29	0.05	-0.17	0.09
(10, 100)	-0.13	0.01	-5.69	0.05	-0.04	0.09
(5, 500)	0.11	0.00	-5.26	0.03	0.12	0.04
(10, 500)	0.01	0.00	-5.51	0.03	0.01	0.04
<i>Student's t</i>						
(5, 50)	-0.12	0.04	-5.59	0.10	-0.07	0.16
(10, 50)	-0.09	0.02	-6.50	0.08	-0.11	0.12
(5, 100)	-0.02	0.02	-5.30	0.06	0.08	0.11
(10, 100)	-0.15	0.01	-6.23	0.06	-0.18	0.09
(5, 500)	0.09	0.00	-5.48	0.03	0.10	0.05
(10, 500)	0.08	0.00	-5.59	0.03	0.09	0.04
<i>Chi-squared</i>						
(5, 50)	1.72	0.07	-5.79	0.12	-0.04	0.20
(10, 50)	0.67	0.04	-6.85	0.09	-0.27	0.15
(5, 100)	1.71	0.03	-5.43	0.07	0.21	0.13
(10, 100)	0.59	0.02	-5.75	0.06	-0.35	0.11
(5, 500)	1.64	0.01	-4.97	0.03	0.02	0.05
(10, 500)	1.05	0.00	-5.22	0.03	0.04	0.05

TABLE B9

Quantile 0.95 and homoscedastic scenario. Average relative bias (%) and root mean squared error (RMSE) for β_4 from the additive quantile mixed model (AQMM) and the additive fixed-effects quantile regression (AFEQR).

Sample size (n, M)	AQMM Rel. bias	AQMM RMSE	AFEQR Rel. bias	AFEQR RMSE
<i>Normal</i>				
(5, 50)	-0.98	0.04	0.25	0.16
(10, 50)	-0.96	0.04	2.39	0.09
(5, 100)	-1.18	0.02	4.13	0.09
(10, 100)	-0.68	0.02	4.18	0.06
(5, 500)	-0.78	0.00	5.31	0.04
(10, 500)	-0.31	0.00	5.21	0.03
<i>Student's t</i>				
(5, 50)	-2.29	0.08	-0.26	0.22
(10, 50)	-1.18	0.05	-0.00	0.11
(5, 100)	-1.46	0.04	1.94	0.10
(10, 100)	-0.98	0.03	1.83	0.06
(5, 500)	-1.60	0.01	4.35	0.03
(10, 500)	-0.63	0.01	4.11	0.03
<i>Chi-squared</i>				
(5, 50)	-6.70	0.30	-10.24	0.49
(10, 50)	-3.23	0.17	-6.72	0.25
(5, 100)	-5.68	0.17	-6.64	0.23
(10, 100)	-3.88	0.10	-4.50	0.13
(5, 500)	-6.42	0.06	-1.05	0.04
(10, 500)	-2.97	0.03	-1.33	0.02

B.2. Heteroscedastic scenario

TABLE B10

Quantile 0.1 and heteroscedastic scenario. Average bias and root mean squared error (RMSE) for $Q(0.1)$ from the additive quantile mixed model (AQMM) and the additive fixed-effects quantile regression (AFEQR). The expected proportion of negative residuals (PNR) is 0.1.

Sample size (n, M)	AQMM			AFEQR		
	PNR	Bias	RMSE	PNR	Bias	RMSE
<i>Normal</i>						
(5, 50)	0.11	-0.15	1.69	0.10	-2.02	3.13
(10, 50)	0.10	-0.25	1.76	0.10	-2.16	3.15
(5, 100)	0.10	-0.15	1.67	0.10	-2.17	3.17
(10, 100)	0.10	-0.25	1.74	0.10	-2.22	3.13
(5, 500)	0.10	-0.17	1.64	0.10	-2.19	3.01
(10, 500)	0.10	-0.26	1.72	0.10	-2.19	3.00
<i>Student's t</i>						
(5, 50)	0.10	-0.63	1.85	0.10	-2.00	3.22
(10, 50)	0.10	-0.61	1.83	0.10	-2.10	3.19
(5, 100)	0.10	-0.54	1.73	0.10	-2.13	3.23
(10, 100)	0.10	-0.55	1.77	0.10	-2.17	3.16
(5, 500)	0.10	-0.54	1.62	0.10	-2.14	3.02
(10, 500)	0.10	-0.54	1.74	0.10	-2.14	3.01
<i>Chi-squared</i>						
(5, 50)	0.09	0.02	1.72	0.10	-1.62	2.94
(10, 50)	0.09	-0.01	1.63	0.10	-1.77	2.93
(5, 100)	0.09	0.01	1.56	0.10	-1.80	2.97
(10, 100)	0.09	-0.03	1.55	0.10	-1.86	2.88
(5, 500)	0.09	0.06	1.38	0.10	-1.85	2.78
(10, 500)	0.10	0.13	1.47	0.10	-1.85	2.77

TABLE B11
Quantile 0.5 and heteroscedastic scenario. Average bias and root mean squared error (RMSE) for $Q(0.5)$ from the additive quantile mixed model (AQMM), the additive fixed-effects quantile regression (AFEQR), and the additive mixed model (AMM). The expected proportion of negative residuals (PNR) is 0.5.

Sample size (n, M)	AQMM			AFEQR			AMM		
	PNR	Bias	RMSE	PNR	Bias	RMSE	PNR	Bias	RMSE
<i>Normal</i>									
(5, 50)	0.50	-0.01	1.62	0.50	-0.01	1.77	0.50	-0.01	1.61
(10, 50)	0.50	-0.00	1.66	0.50	-0.02	1.57	0.50	-0.01	1.66
(5, 100)	0.50	0.01	1.61	0.50	-0.00	1.58	0.50	0.01	1.60
(10, 100)	0.50	-0.00	1.65	0.50	-0.02	1.42	0.50	0.00	1.65
(5, 500)	0.50	0.00	1.59	0.50	-0.02	1.30	0.50	0.00	1.59
(10, 500)	0.50	0.00	1.64	0.50	-0.02	1.29	0.50	0.00	1.64
<i>Student's t</i>									
(5, 50)	0.50	-0.01	1.56	0.50	-0.01	1.89	0.50	-0.01	1.58
(10, 50)	0.50	-0.01	1.56	0.50	-0.04	1.65	0.50	-0.01	1.58
(5, 100)	0.50	0.00	1.50	0.50	-0.01	1.67	0.50	-0.01	1.52
(10, 100)	0.50	0.00	1.54	0.50	-0.02	1.51	0.50	0.00	1.55
(5, 500)	0.50	0.00	1.42	0.50	-0.02	1.36	0.50	0.00	1.43
(10, 500)	0.50	0.00	1.53	0.50	-0.03	1.36	0.50	-0.00	1.53
<i>Chi-squared</i>									
(5, 50)	0.50	1.06	2.23	0.50	0.40	2.19	0.83	3.18	3.55
(10, 50)	0.50	0.99	2.13	0.50	0.36	1.92	0.83	3.20	3.56
(5, 100)	0.50	1.04	2.10	0.50	0.36	1.97	0.83	3.18	3.50
(10, 100)	0.50	0.95	2.05	0.50	0.32	1.75	0.83	3.18	3.51
(5, 500)	0.50	0.98	1.95	0.50	0.30	1.56	0.83	3.19	3.44
(10, 500)	0.50	0.92	1.99	0.50	0.30	1.55	0.83	3.19	3.49

TABLE B12

Quantile 0.95 and heteroscedastic scenario. Average bias and root mean squared error (RMSE) for $Q(0.95)$ from the additive quantile mixed model (AQMM) and the additive fixed-effects quantile regression (AFEQR). The expected proportion of negative residuals (PNR) is 0.95.

Sample size (n, M)	AQMM			AFEQR		
	PNR	Bias	RMSE	PNR	Bias	RMSE
<i>Normal</i>						
(5, 50)	0.94	0.18	1.73	0.95	2.79	3.90
(10, 50)	0.95	0.31	1.81	0.95	2.97	3.99
(5, 100)	0.95	0.22	1.72	0.95	3.02	4.04
(10, 100)	0.95	0.33	1.80	0.95	3.08	4.03
(5, 500)	0.95	0.23	1.68	0.95	3.06	3.94
(10, 500)	0.95	0.35	1.78	0.95	3.06	3.94
<i>Student's t</i>						
(5, 50)	0.95	0.72	2.07	0.95	2.48	3.82
(10, 50)	0.95	0.74	2.06	0.95	2.64	3.85
(5, 100)	0.95	0.65	1.92	0.95	2.69	3.89
(10, 100)	0.95	0.71	1.98	0.95	2.76	3.87
(5, 500)	0.95	0.62	1.77	0.95	2.71	3.74
(10, 500)	0.95	0.66	1.89	0.95	2.72	3.73
<i>Chi-squared</i>						
(5, 50)	0.95	1.73	4.08	0.95	1.15	3.73
(10, 50)	0.95	1.99	4.26	0.95	1.50	3.60
(5, 100)	0.95	1.80	4.07	0.95	1.53	3.63
(10, 100)	0.95	2.00	4.24	0.95	1.64	3.48
(5, 500)	0.95	1.82	3.95	0.95	1.57	3.24
(10, 500)	0.95	1.96	4.11	0.95	1.58	3.21

TABLE B13
Quantile 0.1 and heteroscedastic scenario. Average relative bias (%) and root mean squared error (RMSE) for β_3 from the additive quantile mixed model (AQMM) and the additive fixed-effects quantile regression (AFEQR).

Sample size (n, M)	AQMM Rel. bias	AQMM RMSE	AFEQR Rel. bias	AFEQR RMSE
<i>Normal</i>				
(5, 50)	-0.43	0.69	-7.12	0.54
(10, 50)	-0.48	0.43	-9.88	0.35
(5, 100)	-0.29	0.29	-9.48	0.35
(10, 100)	-3.19	0.14	-9.85	0.23
(5, 500)	-4.14	0.07	-10.40	0.17
(10, 500)	-4.53	0.05	-10.45	0.15
<i>Student's t</i>				
(5, 50)	3.52	0.95	-10.17	0.75
(10, 50)	-0.46	0.56	-10.82	0.44
(5, 100)	-2.96	0.48	-10.93	0.46
(10, 100)	-4.46	0.23	-10.78	0.27
(5, 500)	-5.27	0.11	-11.71	0.20
(10, 500)	-6.34	0.08	-12.47	0.18
<i>Chi-squared</i>				
(5, 50)	3.88	0.85	-7.07	0.68
(10, 50)	1.12	0.45	-9.09	0.54
(5, 100)	0.55	0.34	-9.37	0.52
(10, 100)	-1.97	0.15	-9.97	0.42
(5, 500)	-2.65	0.07	-9.39	0.30
(10, 500)	-2.67	0.05	-10.28	0.33

TABLE B14

Quantile 0.5 and heteroscedastic scenario. Average relative bias (%) and root mean squared error (RMSE) for β_3 from the additive quantile mixed model (AQMM), the additive fixed-effects quantile regression (AFEQR), and the additive mixed model (AMM).

Sample size (n, M)	AQMM		AFEQR		AMM	
	Rel. bias	RMSE	Rel. bias	RMSE	Rel. bias	RMSE
<i>Normal</i>						
(5, 50)	-0.73	0.10	-5.61	0.33	-0.85	0.22
(10, 50)	-0.20	0.05	-5.88	0.19	-0.16	0.15
(5, 100)	0.17	0.05	-5.21	0.17	0.23	0.16
(10, 100)	-0.02	0.02	-5.31	0.10	0.03	0.11
(5, 500)	-0.11	0.01	-5.12	0.07	-0.10	0.07
(10, 500)	0.06	0.00	-5.34	0.06	0.02	0.05
<i>Student's t</i>						
(5, 50)	-0.60	0.17	-5.10	0.36	-0.86	0.36
(10, 50)	-0.29	0.07	-7.07	0.22	-0.44	0.24
(5, 100)	-0.46	0.08	-5.68	0.21	-1.04	0.23
(10, 100)	0.07	0.03	-5.96	0.13	0.30	0.16
(5, 500)	-0.15	0.02	-5.53	0.08	-0.07	0.11
(10, 500)	-0.06	0.01	-6.10	0.07	-0.16	0.08
<i>Chi-squared</i>						
(5, 50)	0.88	0.43	-4.49	0.59	9.25	0.69
(10, 50)	-0.20	0.22	-6.09	0.43	9.47	0.63
(5, 100)	0.71	0.21	-5.66	0.36	9.60	0.65
(10, 100)	-0.14	0.10	-6.14	0.28	9.48	0.61
(5, 500)	0.62	0.04	-5.47	0.17	10.00	0.64
(10, 500)	0.12	0.02	-5.53	0.15	9.83	0.63

TABLE B15
Quantile 0.95 and heteroscedastic scenario. Average relative bias (%) and root mean squared error (RMSE) for β_3 from the additive quantile mixed model (AQMM) and the additive fixed-effects quantile regression (AFEQR).

Sample size (n, M)	AQMM Rel. bias	AQMM RMSE	AFEQR Rel. bias	AFEQR RMSE
<i>Normal</i>				
(5, 50)	-4.48	1.11	-10.65	0.91
(10, 50)	-2.10	0.57	-10.28	0.58
(5, 100)	-0.43	0.50	-10.30	0.59
(10, 100)	0.96	0.23	-8.59	0.34
(5, 500)	2.24	0.09	-7.87	0.21
(10, 500)	1.83	0.05	-7.66	0.17
<i>Student's t</i>				
(5, 50)	-1.36	1.99	-12.09	1.56
(10, 50)	-1.26	0.96	-11.89	0.90
(5, 100)	0.23	0.77	-12.67	0.97
(10, 100)	1.48	0.48	-11.12	0.64
(5, 500)	3.07	0.18	-9.86	0.40
(10, 500)	3.00	0.11	-9.68	0.32
<i>Chi-squared</i>				
(5, 50)	-4.72	5.62	-20.24	8.11
(10, 50)	-4.21	3.14	-16.53	5.23
(5, 100)	-1.14	2.77	-16.28	5.38
(10, 100)	1.24	1.60	-13.81	3.41
(5, 500)	2.20	0.63	-11.84	2.16
(10, 500)	1.86	0.31	-11.44	1.79

TABLE B16

Quantile 0.1 and heteroscedastic scenario. Average relative bias (%) and root mean squared error (RMSE) for β_4 from the additive quantile mixed model (AQMM) and the additive fixed-effects quantile regression (AFEQR).

Sample size (n, M)	AQMM Rel. bias	AQMM RMSE	AFEQR Rel. bias	AFEQR RMSE
<i>Normal</i>				
(5, 50)	1.02	0.04	-16.29	0.34
(10, 50)	-0.04	0.03	-16.38	0.31
(5, 100)	0.92	0.02	-16.24	0.30
(10, 100)	0.24	0.01	-16.16	0.27
(5, 500)	1.23	0.01	-15.97	0.24
(10, 500)	0.35	0.00	-16.31	0.25
<i>Student's t</i>				
(5, 50)	1.44	0.08	-17.81	0.44
(10, 50)	0.77	0.04	-16.87	0.32
(5, 100)	1.17	0.04	-17.22	0.34
(10, 100)	-0.17	0.02	-16.90	0.30
(5, 500)	1.48	0.01	-16.59	0.26
(10, 500)	0.47	0.00	-16.74	0.26
<i>Chi-squared</i>				
(5, 50)	1.40	0.11	-14.22	0.32
(10, 50)	0.58	0.05	-13.90	0.25
(5, 100)	1.13	0.04	-14.35	0.25
(10, 100)	0.28	0.02	-14.62	0.23
(5, 500)	0.77	0.01	-14.20	0.20
(10, 500)	0.10	0.00	-14.52	0.20

TABLE B17

Quantile 0.5 and heteroscedastic scenario. Average relative bias (%) and root mean squared error (RMSE) for β_4 from the additive quantile mixed model (AQMM), the additive fixed-effects quantile regression (AFEQR), and the additive mixed model (AMM).

Sample size (n, M)	AQMM		AFEQR		AMM	
	Rel. bias	RMSE	Rel. bias	RMSE	Rel. bias	RMSE
<i>Normal</i>						
(5, 50)	-0.33	0.03	-5.83	0.10	-0.30	0.14
(10, 50)	-0.27	0.03	-6.77	0.09	-0.38	0.13
(5, 100)	-0.13	0.02	-5.44	0.06	-0.21	0.10
(10, 100)	-0.09	0.01	-5.77	0.05	-0.05	0.09
(5, 500)	0.09	0.00	-5.40	0.03	0.10	0.04
(10, 500)	0.02	0.00	-5.56	0.03	0.01	0.04
<i>Student's t</i>						
(5, 50)	-0.15	0.05	-6.01	0.11	-0.09	0.18
(10, 50)	-0.10	0.03	-6.53	0.08	-0.10	0.14
(5, 100)	-0.18	0.02	-5.36	0.06	0.01	0.13
(10, 100)	-0.12	0.02	-6.25	0.06	-0.17	0.10
(5, 500)	0.11	0.00	-5.49	0.03	0.08	0.06
(10, 500)	0.08	0.00	-5.64	0.03	0.10	0.05
<i>Chi-squared</i>						
(5, 50)	2.03	0.10	-5.38	0.13	-1.06	0.22
(10, 50)	1.12	0.05	-5.88	0.09	-0.32	0.18
(5, 100)	1.97	0.04	-4.77	0.07	-0.26	0.15
(10, 100)	0.92	0.02	-5.03	0.05	-0.45	0.12
(5, 500)	1.99	0.01	-4.41	0.03	0.02	0.07
(10, 500)	1.44	0.01	-4.63	0.03	0.03	0.05

TABLE B18

Quantile 0.95 and heteroscedastic scenario. Average relative bias (%) and root mean squared error (RMSE) for β_4 from the additive quantile mixed model (AQMM) and the additive fixed-effects quantile regression (AFEQR).

Sample size (n, M)	AQMM Rel. bias	AQMM RMSE	AFEQR Rel. bias	AFEQR RMSE
<i>Normal</i>				
(5, 50)	-1.70	0.05	-0.32	0.19
(10, 50)	-0.75	0.04	2.33	0.10
(5, 100)	-1.78	0.03	3.95	0.09
(10, 100)	-0.20	0.02	4.35	0.07
(5, 500)	-1.15	0.01	5.15	0.04
(10, 500)	-0.39	0.00	5.26	0.03
<i>Student's t</i>				
(5, 50)	-2.62	0.13	-1.04	0.27
(10, 50)	-1.35	0.08	0.32	0.14
(5, 100)	-1.55	0.06	1.76	0.12
(10, 100)	-0.79	0.04	2.47	0.08
(5, 500)	-1.57	0.01	4.74	0.04
(10, 500)	-0.61	0.01	4.59	0.03
<i>Chi-squared</i>				
(5, 50)	-5.67	0.39	-5.62	0.51
(10, 50)	-3.28	0.22	-1.00	0.26
(5, 100)	-5.20	0.20	-1.46	0.26
(10, 100)	-4.23	0.13	0.10	0.13
(5, 500)	-5.78	0.06	3.16	0.06
(10, 500)	-3.23	0.03	3.11	0.04

References

ABREVAYA, J. (2001). The effects of demographics and maternal behavior on the distribution of birth outcomes. *Empirical Economics* **26** 247-257.

ANDRIYANA, Y., GIBBELS, I. and VERHASSELT, A. (2014). P-splines quantile regression estimation in varying coefficient models. *Test* **23** 153-194.

ARANDA-ORDAZ, F. J. (1981). On two families of transformations to additivity for binary response data. *Biometrika* **68** 357-363.

AUSTIN, P. C., TU, J. V., DALY, P. A. and ALTER, D. A. (2005). The use of quantile regression in health care research: A case study examining gender differences in the timeliness of thrombolytic therapy. *Statistics in Medicine* **24** 791-816.

BEETS, M. W., WEAVER, R. G., TURNER-MCGRIEVY, G., MOORE, J. B., WEBSTER, C., BRAZENDALE, K., CHANDLER, J., KHAN, M., SAUNDERS, R. and BEIGHLE, A. (2016). Are we there yet? Compliance with physical activity standards in YMCA afterschool programs. *Childhood Obesity* **12** 237-246.

BEYERLEIN, A. (2014). Quantile regression—opportunities and challenges from a user's perspective. *American Journal of Epidemiology* **180** 330-331.

BOX, G. E. P. and COX, D. R. (1964). An analysis of transformations. *Journal of the Royal Statistical Society B* **26** 211-252.

BUCHINSKY, M. (1995). Quantile regression, Box-Cox transformation model, and the US wage structure, 1963-1987. *Journal of Econometrics* **65** 109-154.

BUTTE, N. F., EKELUND, U. and WESTERTERP, K. R. (2012). Assessing physical activity using wearable monitors: Measures of physical activity. *Medicine and Science in Sports and Exercise* **44** S5S12.

CAI, Z. and XU, X. (2008). Nonparametric quantile estimations for dynamic smooth coefficient models. *Journal of the American Statistical Association* **103** 1595-1608.

CAO, Y., CHEN, A., BOTTAI, M., CALDWELL, K. L. and ROGAN, W. J. (2013). The impact of succimer chelation on blood cadmium in children with background exposures: A randomized trial. *The Journal of Pediatrics* **163** 598-600.

CHAMBERLAIN, G. (1994). Quantile regression, censoring, and the structure of wages. In *Advances in Econometrics: Sixth World Congress*, (C. Sims, ed.) **1** Cambridge University Press, Cambridge, UK.

CHEN, C. (2007). A finite smoothing algorithm for quantile regression. *Journal of Computational and Graphical Statistics* **16** 136-164.

CHEN, X., KOENKER, R. and XIAO, Z. (2009). Copula-based nonlinear quantile autoregression. *Econometrics Journal* **12** S50-S67.

CLEVELAND, W. S. (1979). Robust locally weighted regression and smoothing scatterplots. *Journal of the American Statistical Association* **74** 829-836.

CLEVELAND, W. S. and DEVLIN, S. J. (1988). Locally weighted regression: an approach to regression analysis by local fitting. *Journal of the American Statistical Association* **83** 596-610.

COLE, T. J. (1988). Fitting smoothed centile curves to reference data. *Journal of the Royal Statistical Society A* **151** 385-418.

CONTRERAS, M. and RYAN, L. M. (2000). Fitting nonlinear and constrained generalized estimating equations with optimization software. *Biometrics* **56** 1268-1271.

DAVIDIAN, M. and GILTINAN, D. M. (1995). *Nonlinear models for repeated measurement data*. Chapman and Hall/CRC, Boca Raton, FL.

DAVIDIAN, M. and GILTINAN, D. M. (2003). Nonlinear models for repeated measurement data: An overview and update. *Journal of Agricultural, Biological, and Environmental Statistics* **8** 387.

DE BOOR, C. (2001). *A practical guide to splines*. Springer, New York, NY.

DEHBI, H. M., CORTINA-BORJA, M. and GERACI, M. (2016). Aranda-Ordaz quantile regression for student performance assessment. *Journal of Applied Statistics* **43** 58-71.

DEPARTMENT FOR CULTURE, MEDIA AND SPORT (2002). Game plan: A strategy for delivering government's sport and physical activity objectives Technical Report, Cabinet Office, London, UK.

DING, R., MCCARTHY, M. L., DESMOND, J. S., LEE, J. S., ARONSKY, D. and ZEGER, S. L. (2010). Characterizing waiting room time, treatment time, and boarding time in the emergency department using quantile regression. *Academic Emergency Medicine* **17** 813-823.

EFRON, B. and TIBSHIRANI, R. J. (1998). *An introduction to the bootstrap*. Chapman & Hall/CRC, Boca Raton, FL.

EKELUND, U., STEENE-JOHANNESSEN, J., BROWN, W. J., FAGERLAND, M. W., OWEN, N., POWELL, K. E., BAUMAN, A. and LEE, I. M. (2016). Does physical activity attenuate, or even eliminate, the detrimental association of sitting time with mortality? A harmonised meta-analysis of data from more than 1 million men and women. *The Lancet* **388** 1302-1310.

ESPAÑA ROMERO, V., MITCHELL, J. A., DOWDA, M., O'NEILL, J. R. and PATE, R. R. (2013). Objectively measured sedentary time, physical activity and markers of body fat in preschool children. *Pediatric Exercise Science* **25** 154-163.

FAN, R., CHEN, V., XIE, Y., YIN, L., KIM, S., ALBERT, P. S. and SIMONS-MORTON, B. (2015). A functional data analysis approach for circadian patterns of activity of teenage girls. *Journal of Circadian Rhythms* **13** 3.

FENSKE, N., KNEIB, T. and HOTHORN, T. (2011). Identifying risk factors for severe childhood malnutrition by boosting additive quantile regression. *Journal of the American Statistical Association* **106** 494-510.

FENSKE, N., FAHRMEIR, L., HOTHORN, T., RZEHAK, P. and HÖHLE, M. (2013). Boosting structured additive quantile regression for longitudinal childhood obesity data. *The International Journal of Biostatistics* **9** 1-18.

NATIONAL INSTITUTE FOR HEALTH AND CLINICAL EXCELLENCE (2008). National costing report: Physical activity and the environment Technical Report, NICE, London, UK.

NATIONAL INSTITUTE FOR HEALTH AND CLINICAL EXCELLENCE (2009). Promoting physical activity, active play and sport for pre-school and school-age children and young people in family, pre-school, school and community settings Technical Report, NICE, London, UK.

GERACI, M. (2014). Linear quantile mixed models: The lqmm package for Laplace quantile regression. *Journal of Statistical Software* **57** 1-29.

GERACI, M. (2016a). Estimation of regression quantiles in complex surveys with data missing at random: An application to birthweight determinants. *Statistical Methods in Medical Research* **25** 1393-1421.

GERACI, M. (2016b). Qtools: A collection of models and other tools for quantile inference. *The R Journal* **8** 117-138.

GERACI, M. (2017a). Nonlinear quantile mixed models. *ArXiv e-prints*. arXiv:1712.09981v1 [stat.ME].

GERACI, M. (2017b). pawacc: Physical activity with accelerometers. R package version 1.2.2.

GERACI, M. and BOTTAI, M. (2007). Quantile regression for longitudinal data using the asymmetric Laplace distribution. *Biostatistics* **8** 140-154.

GERACI, M. and BOTTAI, M. (2014). Linear quantile mixed models. *Statistics and Computing* **24** 461-479.

GERACI, M. and FARCOMENI, A. (2016). Probabilistic principal component analysis to identify profiles of physical activity behaviours in the presence of nonignorable missing data. *Journal of the Royal Statistical Society C* **65** 51-75.

GERACI, M. and JONES, M. C. (2015). Improved transformation-based quantile regression. *Canadian Journal of Statistics* **43** 118-132.

GERACI, M., RICH, C., SERA, F., CORTINA-BORJA, M., GRIFFITHS, L. J. and DEZATEUX, C. (2012). Technical report on accelerometry data processing in the Millennium Cohort Study Technical Report, University College London.

GILCHRIST, W. (2000). *Statistical modelling with quantile functions*. Chapman & Hall/CRC, Boca Raton, FL.

GREEN, P. and SILVERMAN, B. W. (1994). Nonparametric regression and generalized linear models.

GRIFFITHS, L. J., CORTINA-BORJA, M., SERA, F., POULIOU, T., GERACI, M., RICH, C., COLE, T. J., LAW, C., JOSHI, H., NESS, A. R., JEBB, S. A. and DEZATEUX, C. (2013a). How active are our children? Findings from the Millennium Cohort Study. *BMJ Open* **3**.

GRIFFITHS, L. J., RICH, C., GERACI, M., SERA, F., CORTINA-BORJA, M., POULIOU, T., PLATT, L., JOHNSON, J. and DEZATEUX, C. (2013b). Technical report on the enhancement of Millennium Cohort Study data with accelerometer-derived measures of physical activity and sedentary behaviour in seven year olds Technical Report, Centre for Longitudinal Studies.

GURKA, M. J., EDWARDS, L. J., MULLER, K. E. and KUPPER, L. L. (2006). Extending the Box-Cox transformation to the linear mixed model. *Journal of the Royal Statistical Society A* **169** 273-288.

HASTIE, T. J. and TIBSHIRANI, R. J. (1990). *Generalized additive models*. Chapman and Hall/CRC, New York, NY.

HE, X. M., NG, P. and PORTNOY, S. (1998). Bivariate quantile smoothing splines. *Journal of the Royal Statistical Society B* **60** 537-550.

HOFNER, B., MAYR, A., ROBINZONOV, N. and SCHMID, M. (2014). Model-based boosting in R: A hands-on tutorial using the R package mboost. *Com-*

putational Statistics **29** 3-35.

HOROWITZ, J. L. and LEE, S. (2005). Nonparametric estimation of an additive quantile regression model. *Journal of the American Statistical Association* **100** 1238-1249.

HUANG, Y. and CHEN, J. (2016). Bayesian quantile regression-based nonlinear mixed-effects joint models for time-to-event and longitudinal data with multiple features. *Statistics in Medicine* **35** 5666-5685.

HUTMACHER, M. M., FRENCH, J. L., KRISHNASWAMI, S. and MENON, S. (2011). Estimating transformations for repeated measures modeling of continuous bounded outcome data. *Statistics in Medicine* **30** 935-949.

KARLSSON, A. (2008). Nonlinear quantile regression estimation of longitudinal data. *Communications in Statistics - Simulation and Computation* **37** 114-131.

KATZMARZYK, P. T. and PATE, R. R. (2017). Physical activity and mortality: The potential impact of sitting. *Translational Journal of the American College of Sports Medicine* **2** 32-33.

KLEINER, A., TALWALKAR, A., SARKAR, P. and JORDAN, M. I. (2012). The big data bootstrap. *arXiv preprint arXiv:1206.6415*.

KLEINER, A., TALWALKAR, A., SARKAR, P. and JORDAN, M. I. (2014). A scalable bootstrap for massive data. *Journal of the Royal Statistical Society B* **76** 795-816.

KOENKER, R. (2011). Additive models for quantile regression: Model selection and confidence bandaids. *Brazilian Journal of Probability and Statistics* **25** 239-262.

KOENKER, R. and BASSETT, G. (1978). Regression quantiles. *Econometrica* **46** 33-50.

KOENKER, R. and GELING, O. (2001). Reappraising medfly longevity. *Journal of the American Statistical Association* **96** 458-468.

KOENKER, R. and HALLOCK, K. F. (2001). Quantile regression. *Journal of Economic Perspectives* **15** 143-156.

KOENKER, R. and MIZERA, I. (2004). Penalized triograms: Total variation regularization for bivariate smoothing. *Journal of the Royal Statistical Society B* **66** 145-163.

KOENKER, R., NG, P. and PORTNOY, S. (1994). Quantile smoothing splines. *Biometrika* **81** 673-680.

LINDSEY, J. K. (2001). *Nonlinear models for medical statistics*. Oxford University Press, New York, NY.

LINDSTROM, M. J. and BATES, D. M. (1990). Nonlinear mixed effects models for repeated measures data. *Biometrics* **46** 673-687.

MADSEN, K. and NIELSEN, H. B. (1993). A finite smoothing algorithm for linear l_1 estimation. *Siam Journal on Optimization* **3** 223-235.

MARUO, K., YAMAGUCHI, Y., NOMA, H. and GOSHO, M. (2017). Interpretable inference on the mixed effect model with the Box-Cox transformation. *Statistics in Medicine* **36** 2420-2434.

MORRIS, J. S., ARROYO, C., COULL, B. A., RYAN, L. M., HERRICK, R. and GORTMAKER, S. L. (2006). Using wavelet-based functional mixed models to

characterize population heterogeneity in accelerometer profiles: A case study. *Journal of the American Statistical Association* **101** 1352-1364.

MU, Y. M. and HE, X. M. (2007). Power transformation toward a linear regression quantile. *Journal of the American Statistical Association* **102** 269-279.

MU, Y. M. and WEI, Y. (2009). A dynamic quantile regression transformation model for longitudinal data. *Statistica Sinica* **19** 1137-1153.

MUGGEO, V. M. R., SCIANDRA, M. and AUGUGLIARO, L. (2012). Quantile regression via iterative least squares computations. *Journal of Statistical Computation and Simulation* **82** 1557-1569.

OBERHOFER, W. and HAUPT, H. (2016). Asymptotic theory for nonlinear quantile regression under weak dependence. *Econometric Theory* **32** 686-713.

PINHEIRO, J. C. and BATES, D. M. (1995). Approximations to the log-likelihood function in the nonlinear mixed-effects model. *Journal of Computational and Graphical Statistics* **4** 12-35.

PINHEIRO, J. C. and BATES, D. M. (1996). Unconstrained parametrizations for variance-covariance matrices. *Statistics and Computing* **6** 289-296.

PINHEIRO, J. C. and BATES, D. M. (2000). *Mixed-effects models in S and S-PLUS*. Springer Verlag, New York.

PINHEIRO, J. C. and CHAO, E. C. (2006). Efficient Laplacian and adaptive Gaussian quadrature algorithms for multilevel generalized linear mixed models. *Journal of Computational and Graphical Statistics* **15** 58-81.

PINHEIRO, J., BATES, D., DEBROY, S., SARKAR, D. and R CORE TEAM (2017). nlme: Linear and nonlinear mixed effects models R package version 3.1-131.

R CORE TEAM (2014). R: A language and environment for statistical computing <https://www.R-project.org/>.

REHKOPF, D. H. (2012). Quantile regression for hypothesis testing and hypothesis screening at the dawn of big data. *Epidemiology* **23** 665-7.

REICH, B. J., FUENTES, M. and DUNSON, D. B. Bayesian spatial quantile regression. *Journal of the American Statistical Association* **106** 6-20.

RICH, C., GERACI, M., GRIFFITHS, L. J., SERA, F., DEZATEUX, C. and CORTINA-BORJA, M. (2013). Quality control methods in accelerometer data processing: Defining minimum wear time. *PLoS ONE* **8** e67206.

RICH, C., GERACI, M., GRIFFITHS, L. J., SERA, F., DEZATEUX, C. and CORTINA-BORJA, M. (2014). Quality control methods in accelerometer data processing: Identifying extreme counts. *PLoS ONE* **9** e85134.

RUPPERT, D., WAND, M. P. and CARROLL, R. J. (2003). *Semiparametric regression*. Cambridge University Press, New York.

SERA, F., CORTINA-BORJA, M., GERACI, M., GRIFFITHS, L. J., RICH, C. and DEZATEUX, C. (2011). Modelling accelerometer data from 7-Year old British children using functional analysis of variance. *Journal of Epidemiology and Community Health* **65** (Suppl 2) A26-A27.

SERA, F., GRIFFITHS, L. J., DEZATEUX, C., GERACI, M. and CORTINA-BORJA, M. (2017). Using functional data analysis to understand daily activity levels and patterns in primary school-aged children: Cross-sectional analysis of a UK-wide study. *PLOS ONE* **12** e0187677.

SPOKOINY, V., WANG, W. and HÄRDLE, W. (2013). Local quantile regression. *Journal of Statistical Planning and Inference* **143** 1109-1129.

STURM, R. and DATAR, A. (2005). Body mass index in elementary school children, metropolitan area food prices and food outlet density. *Public Health* **119** 1059-1068.

THOMPSON, P., CAI, Y., MOYEEED, R., REEVE, D. and STANDER, J. (2010). Bayesian nonparametric quantile regression using splines. *Computational Statistics and Data Analysis* **54** 1138-1150.

VONESH, E. F., WANG, H., NIE, L. and MAJUMDAR, D. (2002). Conditional second-order generalized estimating equations for generalized linear and non-linear mixed-effects models. *Journal of the American Statistical Association* **97** 271-283.

WAHBA, G. (1990). *Spline models for observational data*. SIAM, Philadelphia, PA.

WANG, J. (2012). Bayesian quantile regression for parametric nonlinear mixed effects models. *Statistical Methods & Applications* **21** 279-295.

WARBURTON, D. E. R., NICOL, C. W. and BREDIN, S. S. D. (2006). Health benefits of physical activity: The evidence. *Canadian Medical Association Journal* **174** 801-809.

WEI, Y. and TERRY, M. B. (2015). R: "Quantile regression-opportunities and challenges from a user's perspective". *American Journal of Epidemiology* **181** 152-153.

WEI, Y., PERE, A., KOENKER, R. and HE, X. M. (2006). Quantile regression methods for reference growth charts. *Statistics in Medicine* **25** 1369-1382.

WINKELMANN, R. (2006). Reforming health care: Evidence from quantile regressions for counts. *Journal of Health Economics* **25** 131-45.

WOOD, S. N. (2003). Thin plate regression splines. *Journal of the Royal Statistical Society B* **65** 95-114.

WOOD, S. N. (2006a). *Generalized additive models: An introduction with R*. Chapman and Hall/CRC Press, Boca Raton, FL.

WOOD, S. N. (2006b). Low-rank scale-invariant tensor product smooths for generalized additive mixed models. *Biometrics* **62** 1025-1036.

WU, T. Z., YU, K. and YU, Y. (2010). Single-index quantile regression. *Journal of Multivariate Analysis* **101** 1607-1621.

YANG, Y., WANG, H. J. and HE, X. (2016). Posterior inference in Bayesian quantile regression with asymmetric Laplace likelihood. *International Statistical Review* **84** 327344. doi:10.1111/insr.12114.

YU, K. and JONES, M. C. (1998). Local linear quantile regression. *Journal of the American Statistical Association* **93** 228-237.

YUE, Y. R. and RUE, H. (2011). Bayesian inference for additive mixed quantile regression models. *Computational Statistics & Data Analysis* **55** 84-96.